# CHAPTER IV
# CATALYTIC EXTRUSION OF POLYLACTIDE/ETHYLENE VINYL ALCOHOL BIOPLASTIC FILM

## 4.1 ABSTRACT

The ring opening polymerization of lactide was generated by a continuous single-step reactive extrusion process in the presence of 2-ethylhexanoic acid tin(II) salt, $Sn(Oct)_2$, as a catalyst to obtain high molecular weight polylactide (PLA). For good practical applications of PLA, the softness of the PLA was modified via the graft copolymerization from poly(ethylene-co-vinyl alcohol) EVOH, which is a bio-compatible, flexible and soft random copolymer. To investigate the chemical structure of the graft copolymer, the products were characterized by FTIR. The results show that the strong absorption emerged at 1740 $cm^{-1}$ in the spectra of EVOH-g-PLA and pure PLA was identical, which assigned to carbonyl (C=O) in PLA. Therefore, these results could be confirmed that the ring-opening polymerization of lactide with EVOH by using catalytic extrusion was carried out successfully. Furthermore, the EVOH-g-PLA copolymers gave the number average molecular weight ($M_w$) ranging from $24.5 \times 10^4$ to $36.6 \times 10^4$ g/mol. The amount of graft copolymer and the grafting degree showed a maximum at a catalyst concentration around 0.5 wt%. The optimized LA/EVOH content and the screw speed were 60/40 wt% and 30 rpm, respectively. Furthermore, the EVOH-g-PLA copolymers were fabricated into bioplastic films by compression moulding technique for morphological study by SEM and mechanical testing. The elongation of grafted PLA were improved significantly compared to pure PLA. The tradeoff included the reduction of tensile strength.

Keywords: reactive extrusion, polylactide, ring-opening polymerization

## 4.2 INTRODUCTION

Worldwide, the problems associated with the production of large amounts of waste are recognized as one of the most serious one has to face in the following centuries. In the case of plastic waste the preferred solution, up to now, is recycling. Nevertheless, degradable materials can play an important role to reduce these waste

disposal problems [1]. Polymers from renewable resources have attracted an increasing amount of attention over the last two decades, predominantly due to environmental concerns. Generally, polymers from renewable resources can be classified into three groups: (1) natural polymers, such as starch, protein and cellulose; (2) synthetic polymers from natural monomers, such as polylactide (PLA); and (3) polymers from microbial fermentation, such as polyhydroxybutyrate (PHB) [2].

Polylactide (PLA), a hydrolyzable aliphatic polyester known and used for a long time for medical applications (tissue engineering, bone fixation, and controlled drug delivery). PLA is the one of commercially available biobased materials that could become a material of choice, especially in packaging applications due to its good clarity, high strength and moderate barrier properties [3]. PLA is prepared by two ways, the polycondensation of lactic acid and the ring-opening polymerization of lactide. Higher molecular weight PLA is usually prepared by ring-opening pathway than polycondensation pathway [1,4] and cost of PLA is high due to expensive lactide. Nevertheless, PLA is stiff and brittle. The brittleness causes a problem in processsibility and high crystallinity reduces it rates of decomposition [5]. Therefore, PLA needs modification to moderately enhance the flexibility, improve the strength and processibility, increase the rate of decomposition for decreasing the global warming, and reduce the cost.

To overcome these limitations of PLA, grafting brittle polymer on copolymers is of great interest for developing polymeric materials, i.e. grafting copolymerization of PLA with poly(glycolic acid) (PGA) is a possible method to enhance the rate of degradation by disturbing the crystallinity of PLA [5]. Moreover, the plasticization of PLA is a method to improve the mechanical properties. Starch/PLA blends has focused on the incorporation of dry starch into PLA to reduce the cost of the material while maintaining biodegradability. Blending of PLA with thermoplastic starch leads to blends with greatly improved ductility [6]. However, some plasticizers lead to leak or bloom. In 2000, Jacobsen S. studied the ring-opening polymerization of lactide by using catalytic extrusion with $Sn(Oct)_2$ as a catalyst. The resulting conversion was 99 %, indicating the complete reaction. This single-step reactive extrusion process required the shorter time to reach this conversion than the case of classical batch process [1].

All above ideas lead to the purpose of this research, the improvement of bioplastic PLA by grafting-from method via catalytic extrusion with Sn(Oct)$_2$ as a catalyst in order to make the production of PLA economically viable, enhance flexibility, and increase the degradation rate. Ethylene vinyl alcohol copolymer (EVOH) which has the reactive hydroxyl groups is a good backbone used to initiate the ring-opening polymerization of lactide. This leads to the high molecular weight of resulting polymer because EVOH backbone has high molecular weight and uses the higher content of PLA than backbone to generate the matrix of PLA. Furthermore, due to EVOH is the material that has water resistance, biodegradability, and good barrier properties, this could be benefit for the graft copolymer to be used in packaging applications.

Thereby, this work is focused on the processing parameter which is the screw speed influenced on the reaction time and mixing efficiency, LA/EVOH content affected to the morphology and compatibility between two components, and catalyst content gave the high conversion and the outstanding properties of resulting products.

## 4.3 EXPERIMENTAL

### Materials

L-lactide ((3$S$)-$cis$-3,6-Dimethyl-1,4-dioxane-2,5-dione) was purchased from Bio Invigor Corporation Co., Ltd., Ethylene Vinyl Alcohol copolymer with 68 mol % Vinyl Alcohol Copolymer (EVAL F171, 1.8 MFI) was purchased from Kurarey., 2-ethylhexanoic acid Tin (II) (Sn(Oct)$_2$) was supplied by Sigma., Zinc Stearate (Zn(C$_{17}$H$_{35}$COO)$_2$) and Calcium Stearate (Ca(C$_{17}$H$_{35}$COO)$_2$) were ordered from Imperial Industrial Chemical Co., Ltd.

Chloroform (CHCl$_3$), isopropyl alcohol, and dimethylformamide (DMF) were purchased from Lab Scan Co., Ltd.

### Synthesis of PLA with EVOH by solution ring-opening polymerization

Ring-opening polymerization of lactide was conducted using stannous octoate (Sn(Oct)$_2$) as catalyst. The 10 g EVOH was dissolved in 40 ml toluene and heat

at 185 °C. This mixture was placed in a round bottom flask, together with 15 g lactide monomer and solution of 0.1 wt%. $Sn(Oct)_2$ catalyst. The round bottom flask was sealed and conditioned in oil bath kept at a temperature of 200 °C and vigorously shaken until the monomer was melted and the catalyst was completely mixed with the molten monomer. Then the reaction was operated about 24 h. After that the reaction was stopped by quenching to room temperature. The reacted solution was opaque. The polymerization product was precipitated with dichloromethane for chemical analysis by FTIR spectrometer.

**Synthesis of PLA with EVOH by using Brabender Mixer W50**

For ring-opening polymerization, the mixture of lactide monomer (50 wt%) and EVOH (50 wt%) mixed with 0.1 wt% of $Sn(Oct)_2$ and 5 wt% of Zn/Ca stearate stabilizer was placed in the chamber used as polymerization reactor and purged with $N_2$ gas. Firstly, 25 g EVOH and $Sn(Oct)_2$ were added to the chamber and mixed for 3 min. Then the 25 g lactide and 2.5 g Zn/Ca stearate (50/50 wt%) were added and mixed further for 30 min. The operating temperatures were varied at 185, 195, and 205 °C. The rotor speeds were maintained at 40 and 60 rpm. The crude graft copolymer was characterized for chemical analysis by FTIR spectrometer.

**Synthesis of PLA with EVOH by using twin-screw extruder**

For reactive extrusion polymerization, the lactide monomer and EVOH are used as received without further purification. A mixture of lactide, EVOH, 0.1 wt% of $Sn(Oct)_2$ catalyst, and 5 wt% of Zn/Ca stearate stabilizer were shaken by powder mixer. The prepared mixture is transferred into a Collin D-8017 T20 co-rotating twin-screw extruder, having a screw diameter of 25 mm and a L/D ratio 30, as polymerization device. The temperatures were set from hopper to die as 80, 160, 190, 220, 220, and 220 °C, respectively. The polymer is extruded through a round die and pelletised. The screw speed (30, 40, 50, and 60 rpm), LA/EVOH content (50/50, 60/40, 70/30, and 80/20 wt%), and catalyst content (0.1, 0.3, and 0.5 wt%) are varied. The crude graft copolymer was characterized by FTIR, DSC, TGA, XRD, DMA, and tensile testing.

**Soxhlet extraction**

The resulting polymers obtained from the reactive extrusion were purified by extraction with isopropyl alcohol at the temperature of about 183 °C for 3 h or with chloroform at the temperature about 160 °C for 3 h. After that the resulting yields were dried in vacuum oven at the temperature of 85 °C for the extracted polymer with isopropyl alcohol and 60 °C for the extracted polymer with chloroform. Then the extracted polymers were characterized by FTIR spectrometer and NMR for studying the chemical structure and calculating the amount of the graft copolymer and homopolymer, conversion, and degree of grafting.

**Preparation of bioplastic films**

The crude polymers obtained from bulk twin screw extruder were prepared into thin film with 0.35 mm thickness by using a Labtech compression moulding machine with preheating for 5 min, followed by heating for 20 min at a force of 25 kN. The operating temperatures of mould were maintained at 200 °C and cooled down to room temperature. Then these thin films were used to study the color intensity. Moreover, the crude polymers were prepared into the sheet of 3 mm thickness by using a Labtech compression moulding machine with the method which was similar to the former method. After that, these sheets were cut into dumbbell-shape for investigating the tensile properties and bar-shape for investigating the dynamic-mechanical property.

**Physical Measurements**

DSC analyses were carried out by using a Perkin-Elmer DSC 7 instrument. The samples were first heated from -20°C to 200 °C and cooled down with a flow rate of 10 ml/min. The samples was then reheated to 200°C at the same rate.

X-ray diffraction profiles were measured on a Rigaku Model Dmax 2002 diffractometer with Ni-filtered Cu $K_{\alpha}$ radiation operated at 40 kV and 30 mA. The film samples were observed on the 2θ range of 2-30 degrees with a scan speed of 2 degrees/min and a scan step of 0.02 degrees.

DMA analyse were carried out by using a dynamic-mechanical analyzer GABO EPLEXOR QC 25 instrument. The samples were 13 mm x 55 mm x 3 mm (width x length x thickness). The testing temperature was -30 to 100 °C, 10 Hz for frequency. Static and dynamic strains were 3 % and 1.5 %, respectively. The tension mode was used.

TG-DTA curves were collected on a Perkin-Elmer Pyris Diamond TG/DTA instrument. The samples were loaded on the platinum pan and heated from 50°C to 550 °C at a heating rate of 10°C/min under $N_2$ flow of 100 mL/min.

Scanning electron microscopy was performed on JEOL JSM-5410 Model to observe the morphology of the samples. The extrudates obtained from twin-screw extruder were broken in liquid nitrogen. All of the specimens were coated with gold under vacuum before observation to make them electrically conductive.

Gel Permeation Chromatography (GPC) Shimadsu Model was carried out in DMF solvent as the mobile phase using KD-806 M column and RID-10A detector. The DMF solvent was filtrated with MN 615 $\varnothing$ 155 mm filter paper under the vacuum. The crude polymers were dissolved in DMF at the concentration 0.5 wt% and filtrated with 0.45 mm diameter of cellulose acetate filter before injecting into the column. The conditions of this machine were 40-85 °C column temperature, 1 ml/min flow rate, and 30 min run time. Molecular weight and molecular weight distribution of PLA were calculated in reference to a polystyrene calibration.
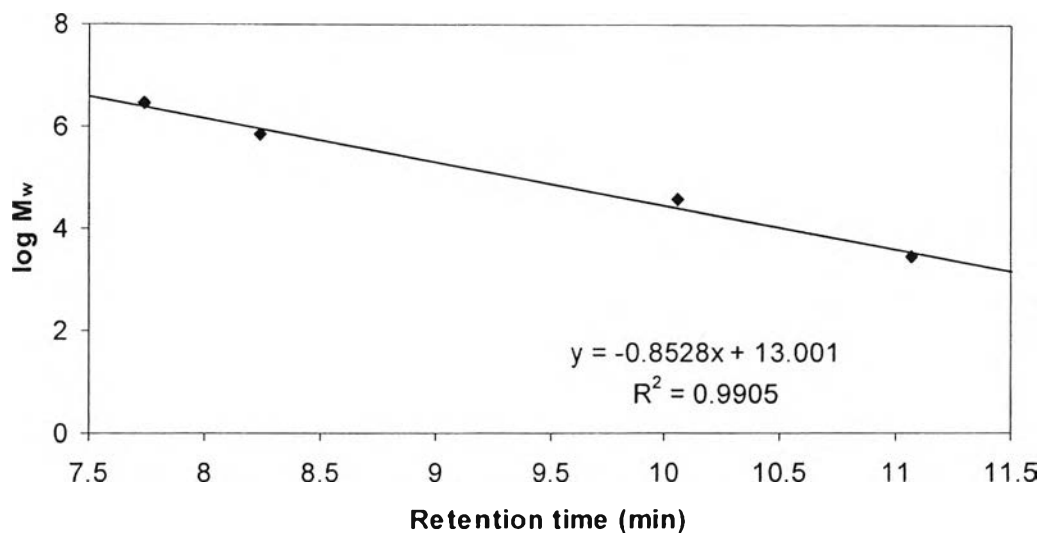
**Figure 4.3.1** The polystyrene calibration for the calculation of molecular weight.

**Chemical Analysis**

Infrared spectra of EVOH-g-PLA copolymers were recorded on a Nicolet Nexus 670 FT-IR spectrometer in the frequency range of 4000-400 cm$^{-1}$ with 32 scans at a resolution of 4 cm$^{-1}$. Samples were prepared by casting 0.05 wt% chloroform solutions on KBr pellets, followed by vacuum drying at 50 °C for 48 h. The presenting the C=O groups in LA ring is investigated and the conversion is calculated by using FTIR.

$$c \quad = \quad 1 - ([LA]/[LA]_0)$$

where [LA] is the amount of residual lactide and $[LA]_0$ is the amount of initial lactide.
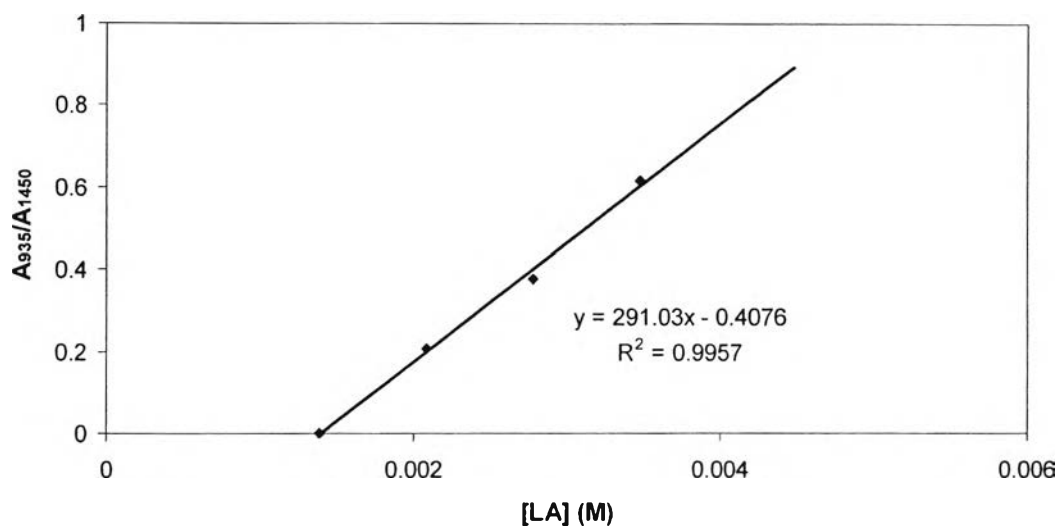
**Figure 4.3.2** The calibration curve for the calculation of lactide conversion.

In addition, the degree of grafting is calculated by using FTIR. Infrared spectra of isopropyl alcohol extracted EVOH-g-PLA copolymers were recorded on a Nicolet Nexus 670 FT-IR spectrometer in the frequency range of 4000-400 cm$^{-1}$ with 32 scans at a resolution of 4 cm$^{-1}$. Samples were prepared by casting 0.05 wt% chloroform solutions on KBr pellets for 0.1 ml, followed by vacuum drying at 50 °C for 48 h. The presenting the OH groups is investigated.

Grafting degree (%) = $(1 - (\text{mole of } OH_r/\text{mole of } OH_i)) \times 100$

where $OH_r$ was the residual O-H group after extraction with isopropyl alcohol and $OH_i$ was the initial O-H group before extraction with isopropyl alcohol.
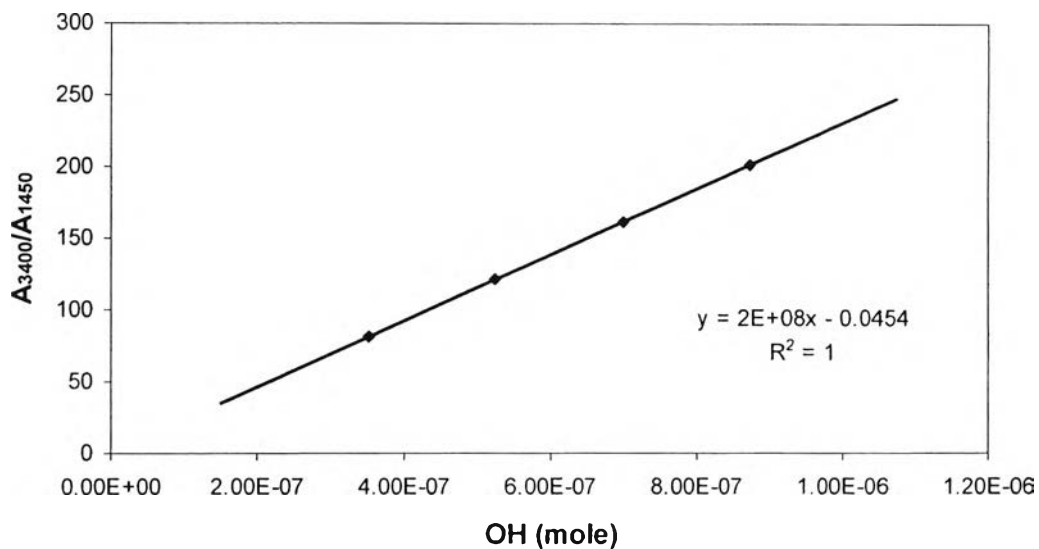
**Figure 4.3.3** The calibration curve for the calculation of grafting degree.

$^1$H NMR measurement, the samples were dissolved in DMSO-d$_6$ in 5 mm NMR tubes at room temperature. The sample concentration was about 1.0 % by weight. NMR spectra were recorded on a Varian XL-300 NMR spectrometer working at 300.032 MH$_z$ for protons.

**Mechanical Testing**

The tensile properties were tested by using an Instron 4206 Universal Testing Machine with cross-head speed of 50 mm/min. The samples were in the dumbbell-shape. The size of sample specimen was 13 mm width of narrow section, 90 mm length of narrow section, and 3 mm thickness.

## 4.4 RESULTS AND DISCUSSION

## Characterization of EVOH-g-PLA obtained from solution polymerization

### 4.4.1 Chemical analysis

Figure 4.1 shows FTIR spectra of EVOH-g-PLA (50/50 wt% LA/EVOH content, and 0.1 wt% catalyst) synthesized by solution polymerization in comparison with the spectra of EVOH. The strong absorption of the peak at 1740 cm$^{-1}$ assigned to (C=O) carbonyl group of branched PLA as a result of grafting. This indicated that the ring-opening polymerization of lactide by using the reactive hydroxyl group (-OH) of EVOH and Sn(Oct)$_2$ as a catalyst was possible in solution polymerization.
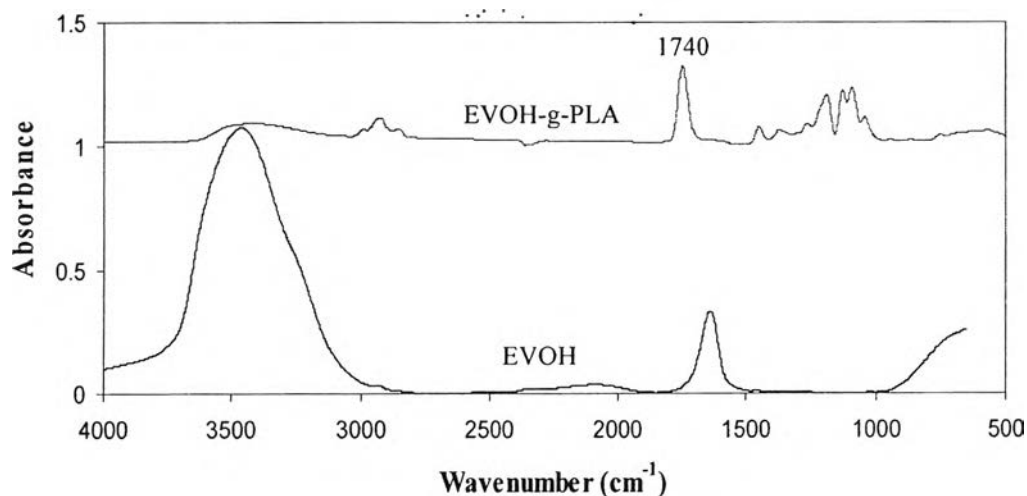


**Figure 4.1** FTIR spectra of EVOH and EVOH-g-PLA (50/50 wt %) obtained from solution polymerization.

## Characterization of EVOH-g-PLA obtained from brabender mixer

### 4.4.2 Fusion behavior

Figures 4.2, 4.3, and 4.4 showed the evolution of torque and temperature as a function of time for different rotor temperatures and rotor speed. The melt-

ing process corresponded to the first peak of the torque histogram. The maximum torques observed at the temperature of about 185 °C and the rotor speed of about 40 and 60 rpm were 39 and 60 Nm respectively (Figure 4.2). The maximum torques of the resulting polymers operated at the temperature of about 195 °C and the rotor temperature of about 40 and 60 rpm were 44 and 44.5 Nm respectively (Figure 4.3). Finally, the maximum torques of the resulting polymers operated at the temperature of about 205 °C and the rotor temperature of about 40 and 60 rpm were 49 and 50 Nm, respectively (Figure 4.4). The torque value then went down quickly to zero. A maximum value was reached after 2 min. It started to increase after 12 min, indicating that the polymerization of lactide proceeded. A maximum value was reached after about 18 min of mixing. These values were very low because of low viscosity of the mixtures, especially the monomer. For the reaction operated at 205 °C (Figure 4.4), the polymers were degraded before the polymerization was finished. On the hand, by considering reaction temperature, it follows that after adding cool EVOH and monomer, temperature decreases and then raises up after 4 min, approximately. By increasing screw speed, temperature rising shifts to start at slightly longer time. This suggests that reaction is readily occurred and may take about 12-18 min to finish. The effect of screw speed at 185 °C on final viscosity is hardly seen since the final reaction torques and temperature for both speeds are not significantly different. Thus, the extent of reaction by both rotor speeds could be similar. However, at higher temperature 195 and 205 °C, it is likely that lower speed 40 rpm induces more increase in torque and temperature, suggesting more extent of reaction than 60 rpm rotor speed.

The results in Figures 4.2 and 4.3 showed that the ring-opening polymerization of lactide monomer could be completely generated in the brabender mixer at overall of these studied conditions. This was confirmed by FTIR spectra (Figure 4.6). The maximum torques of resulting polymers were not much higher than that of the rotor in brabender mixer could stand. However, the appearance of the resulting polymers was different especially in their color shown in Figure 4.5. The color of the polymers generated at the temperature of 205 °C was dark yellow, whereas that of the polymers generated at the temperature less than 200 °C was

rather white. This reveals that the operating temperature higher than 200 °C causes the degradation of these resulting polymers.
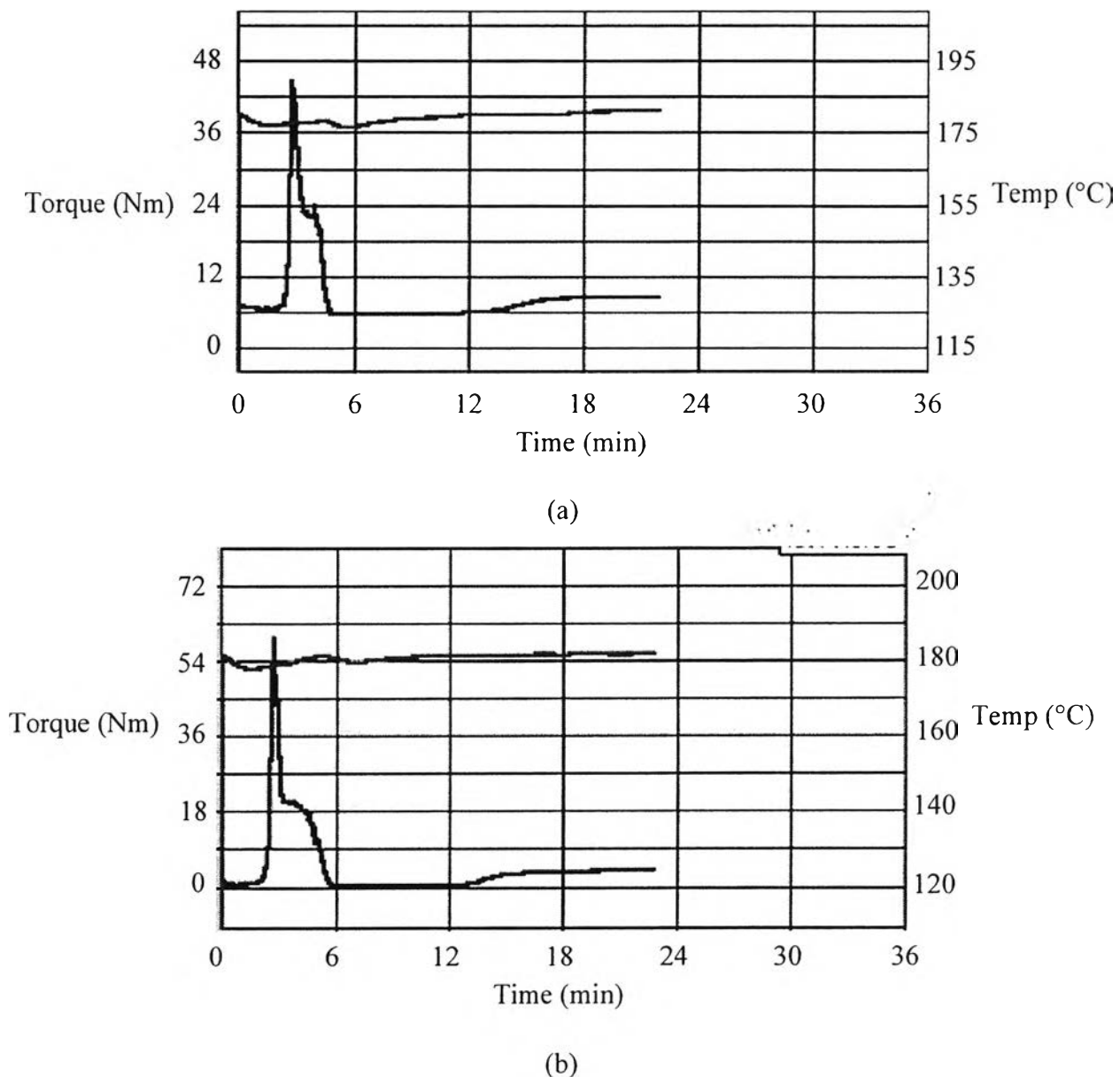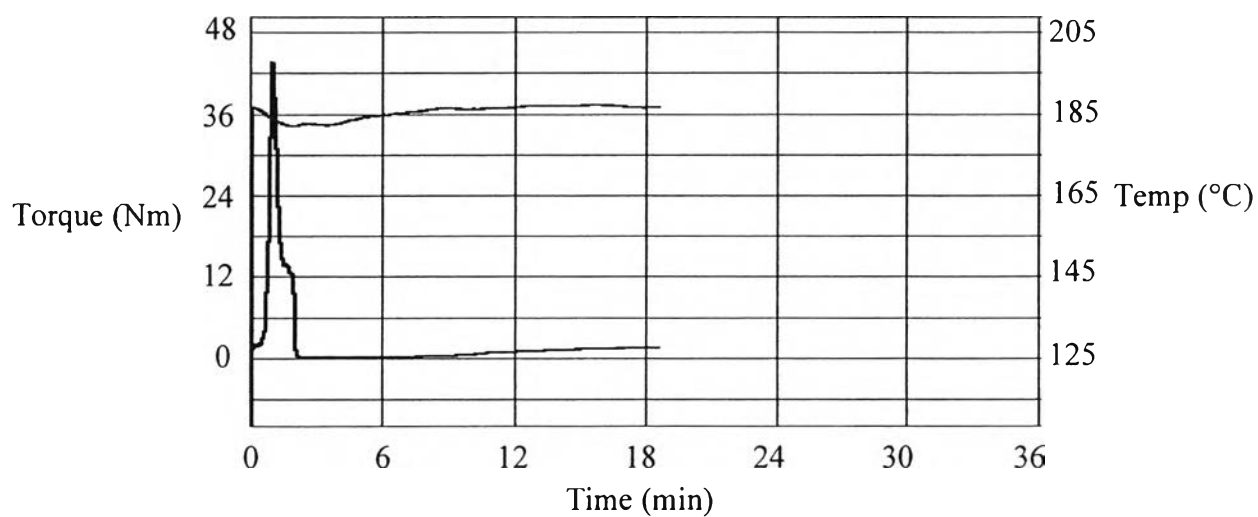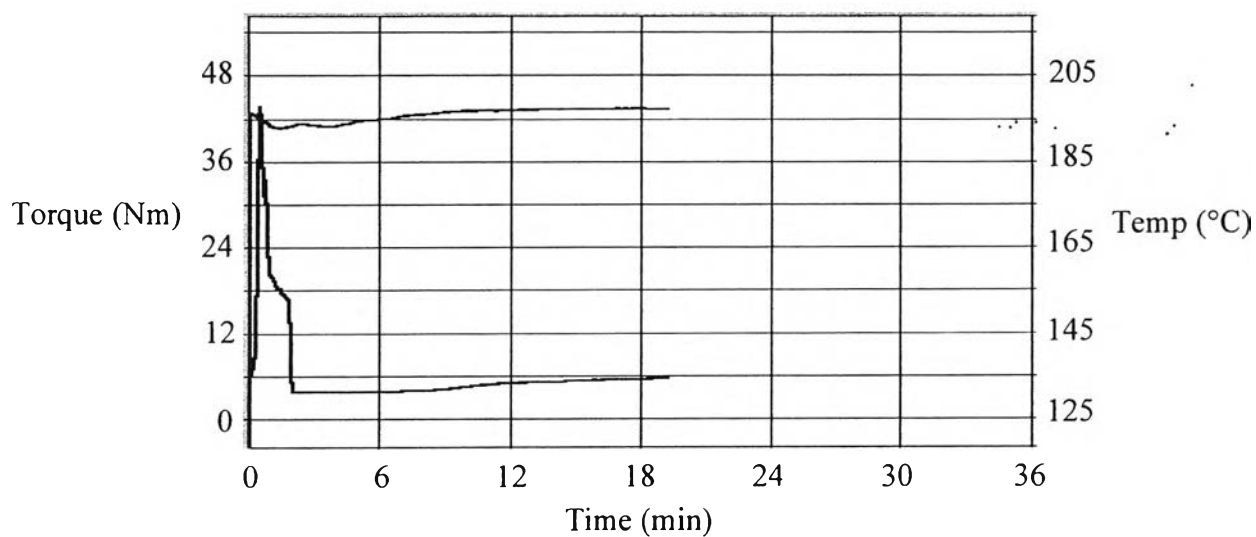


(a)



(b)

**Figure 4.2** Fusion behavior of crude EVOH-g-PLA (50/50 wt%) in the presence of 0.1 wt% $Sn(Oct)_2$ catalyst and 5 wt% Zn/Ca stearate stabilizer operated at 185 °C of chamber temperature and the rotor speed at (a) 40 rpm and (b) 60 rpm.
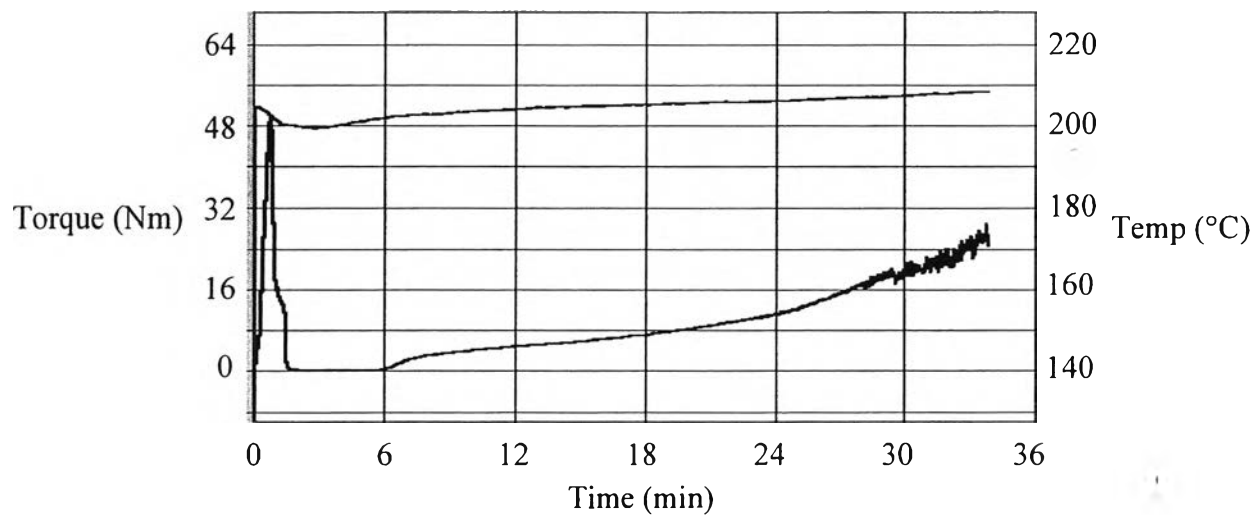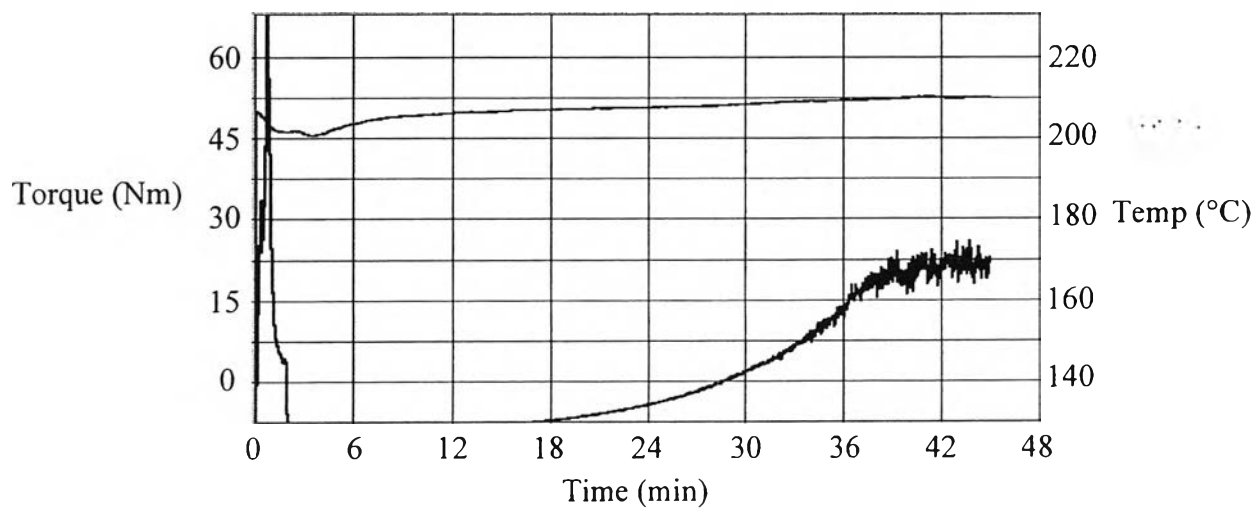
(a)



(b)

**Figure 4.3** Fusion behavior of crude EVOH-g-PLA (50/50 wt%) in the presence of 0.1 wt% Sn(Oct)$_2$ catalyst and 5 wt% Zn/Ca stearate stabilizer operated at 195 °C of chamber temperature and the rotor speed at (a) 40 rpm and (b) 60 rpm.

(a)



(b)

**Figure 4.4** Fusion behavior of crude EVOH-g-PLA (50/50 wt%) in the presence of 0.1 wt% $Sn(Oct)_2$ catalyst and 5 wt% Zn/Ca stearate stabilizer operated at 205 °C of chamber temperature and the rotor speed at (a) 40 rpm and (b) 60 rpm.
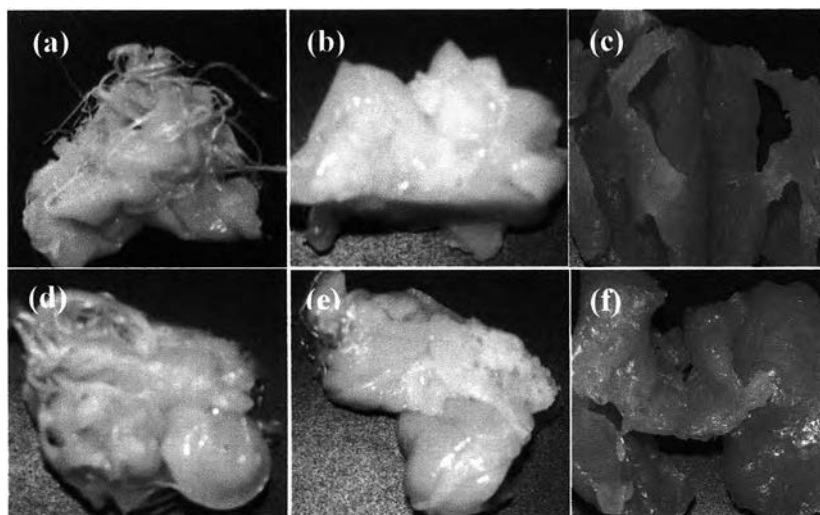
**Figure 4.5** The appearance of crude EVOH-g-PLA synthesized by using a brabender mixer with 50/50 LA/EVOH content (wt%), catalyzed with 0.1 wt% $Sn(Oct)_2$ and stabilized with 5 wt% Zn/Ca stearate at 40 rpm rotor speed (a) 185 °C, (b) 195 °C, and (c) 205 °C rotor temperature and 60 rpm rotor speed (d) 185 °C, (e) 195 °C, and (f) 205 °C.

### 4.4.3 Chemical analysis

FTIR spectra of EVOH, LA and crude EVOH-g-PLA (50/50 wt%) obtained from brabender mixer are shown in Figure 4.6. Compared the spectrum of EVOH with crude EVOH-g-PLA at both 185 and 195 °C varied rotor temperatures, the strong absorption emerged at 1740 $cm^{-1}$ in the spectra of both of crude EVOH-g-PLA and PLA homopolymer , assigned to carbonyl (C=O) in branched PLA as a result of the grafting and PLA homopolymer. The 1188 and 1215 $cm^{-1}$ doublets observed in the crude polymer are assigned to the symmetric C–O–C stretching modes of the ester group. There are two other peaks at 1130 and 1045 $cm^{-1}$ attributed to the methyl rocking and C–$CH_3$ stretching, vibration, respectively. These results could be concluded that the ring-opening polymerization of lactide and grafting from EVOH were generated in the brabender mixer at both rotor temperatures.
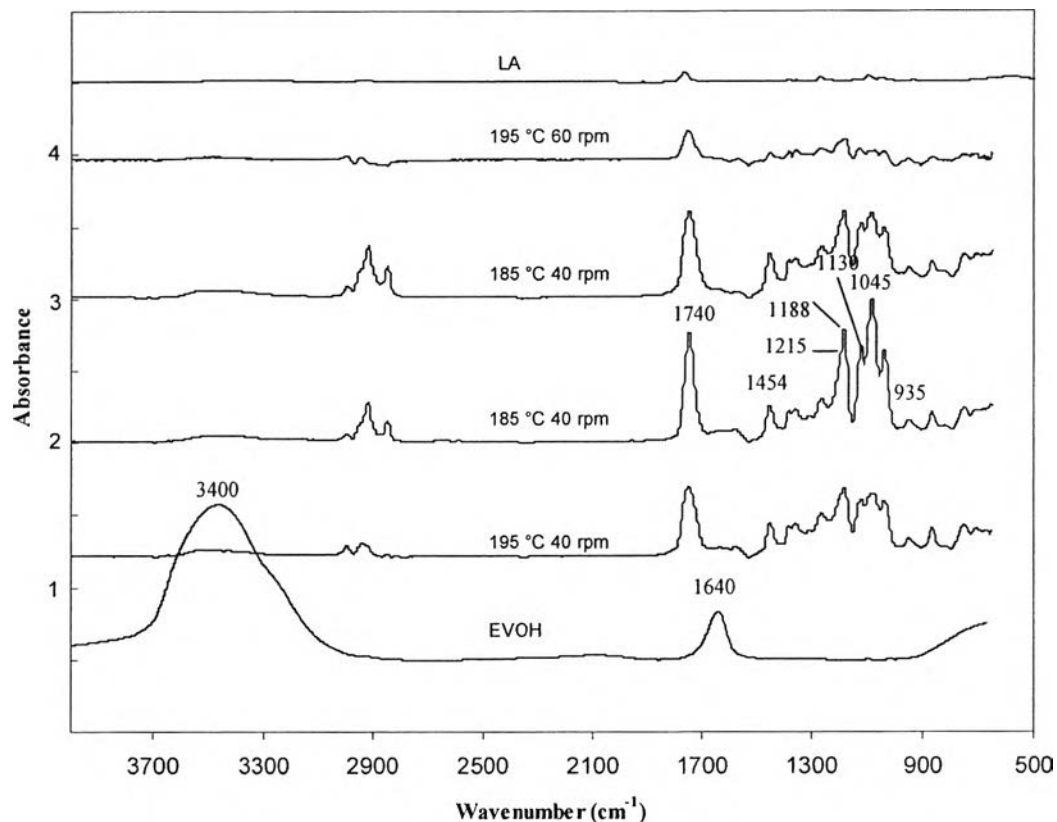
**Figure 4.6** FTIR spectra of EVOH and crude EVOH-g-PLA (50/50 wt%) obtained from brabender mixer at 40 rpm rotor speed.

**Characterization of EVOH-g-PLA obtained from twin-screw extruder**

4.4.4 The Amount of Graft Copolymer

After purification by using soxhlet extraction with chloroform, the amount of EVOH-g-PLA copolymer was calculated by using following equation and shown in Table 4.1.

Grafting content = Weight of insoluble product (g)/weight of crude product (g)   (1)

**Table 4.1** The amount of graft copolymer and homopolymer of PLA after extraction crude graft copolymer with chloroform

| Samples | Composition (%) | |
|---|---|---|
| | Graft copolymer (Insoluble part) | Homopolymer (Soluble part) |
| **LA/EVOH content (wt%)** | | |
| (0.1 wt% catalyst) | | |
| 40 rpm | | |
| 50/50 | 74.72 | 23.30 |
| 60/40 | 77.54 | 20.36 |
| 70/30 | 46.45 | 32.25 |
| 80/20 | 13.86 | 73.93 |
| 30 rpm | | |
| 60/40 | 57.99 | 28.11 |
| 70/30 | 60.36 | 23.96 |
| 80/20 | 4.68 | 61.54 |
| **Screw Speed (rpm)** | | |
| (60/40 wt% LA/EVOH, 0.1 wt% catalyst) | | |
| 30 | 57.99 | 28.11 |
| 40 | 77.54 | 20.36 |
| 50 | 59.91 | 24.88 |
| 60 | 42.22 | 29.02 |
| **Catalyst Content (wt%)** | | |
| (60/40 wt% LA/EVOH, 30 rpm) | | |
| 0.1 | 57.99 | 28.11 |
| 0.3 | 70.22 | 24.61 |
| 0.5 | 75.68 | 0.19 |

Table 4.1 shows the dependence of grafting content on LA/EVOH contents, catalyst contents, and screw speeds. Increase in LA/EVOH contents resulted in the reduction of the content of graft copolymer which related to the amount of free hydroxyl groups in the EVOH backbone [5] and viscosity of lactide and EVOH. In this case, the LA/EVOH content at 60/40 wt% gave the highest yield of graft copolymer. The graft copolymer contents varied with the screw speeds and catalyst contents are less significant on grafting content than LA/EVOH contents. Varying screw speed alters the grafting content between 42-77 % while increasing catalyst content leads to enhancing grafting content from 58-77 %. An optimum is at screw speed 40 rpm. When increased the screw speeds from 30 to 60 rpm, the yield of graft copolymer decreased. The remaining residence time inside the twin-screw extruder decreased with increasing screw speed, as a result, the reaction time could be too short to complete the reaction [1]. Moreover, increasing the catalyst content from 0.1 to 0.5 wt%, the yield of graft copolymer increased and increased up to 76 % in the case of 0.5 wt% catalyst content. Noticeably, from Table 4.1, there is another component, which was the difference between 100 % of all compositions and the combination of the component of graft copolymer and homopolymer, estimating the amount of graft copolymer that adhered in the timple. This is the error in the extraction.

### 4.4.5 Yield of reacted EVOH

After extraction the crude sample with isopropyl alcohol to remove non-reacted EVOH, % yield of all products was calculated by using following equation and shown in Table 4.2.

% yield = [Weight of insoluble product (g)/Weight of crude product (g)] x 100    (2)

**Table 4.2** % yield of reacted EVOH after extraction the crude sample with isopropyl alcohol

| Samples | % Yield (by weight) of reacted EVOH (Insoluble Part) |
|---|---|
| **LA/EVOH content (wt %)** | |
| (0.1 wt% catalyst) | |
| <u>40 rpm</u> | |
| 50/50 | 31.7 |
| 60/40 | 37.4 |
| 70/30 | 31.3 |
| . 80/20 | 32.0 |
| <u>30 rpm</u> | |
| 60/40 | 46.0 |
| 70/30 | 40.5 |
| 80/20 | 50.8 |
| **Screw speed (rpm)** | |
| (60/40 wt% LA/EVOH, 0.1 wt% catalyst) | |
| 30 | 46.0 |
| 40 | 37.4 |
| 50 | 41.0 |
| 60 | 42.0 |
| **Catalyst Content (wt%)** | |
| (60/40 wt% LA/EVOH, 30 rpm) | |
| 0.1 | 46.0 |
| 0.3 | 44.1 |
| 0.5 | 56.7 |

However, isopropyl alcohol can dissolve the graft copolymer except non-reacted EVOH. The evidence could be seen from the FTIR spectra that showed the absorption peak of carbonyl group of PLA in the extracted sample (Figure 4.7). Therefore, the yields of EVOH-g-PLA may be underestimated. But at 80/20 wt% LA/EVOH content the yield of reacted EVOH could be overestimated due to the homopolymer content. From Table 4.2, it also suggests that among three parameters the effect of LA/EVOH content is more significant on grafting content or % yield of reacted EVOH than screw speed and catalyst content.
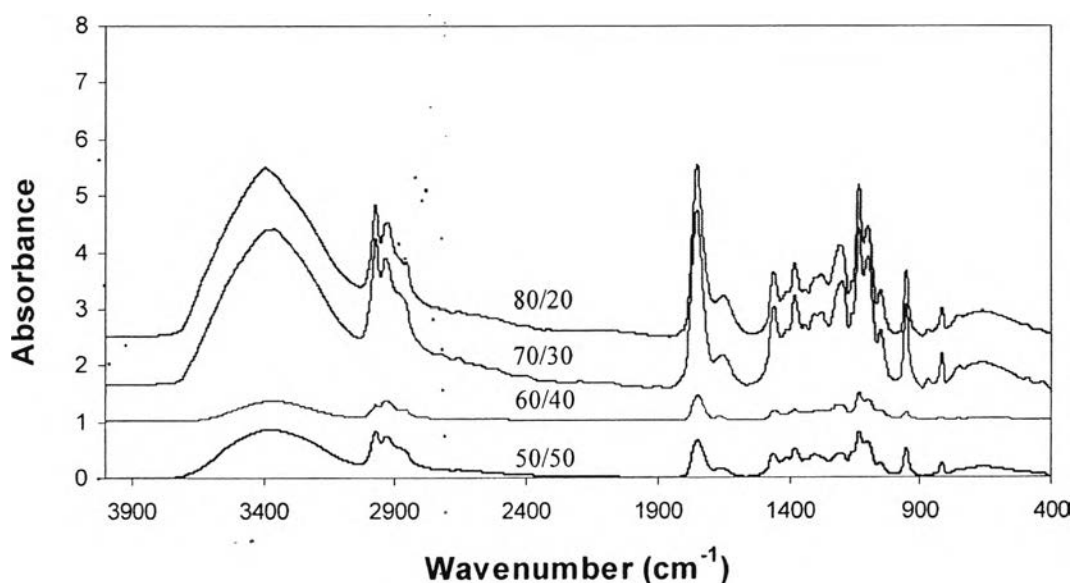


**Figure 4.7** FTIR spectra of soluble part after extraction crude graft copolymers with isopropyl alcohol.

### 4.4.6 Chemical analysis

In Figure 4.8, compared the spectrum of EVOH with graft copolymer obtained from the catalytic extrusion, the absorption emerged at the same peak as the FTIR spectra in Figure 4.5 which is the FTIR spectra of graft copolymer obtained from brabender mixer. The absorption peak at 935 cm$^{-1}$ which is the characteristic of lactide ring was observed in the spectra of graft copolymer but its intensity was much lower than its intensity in the spectra of lactide. This meant that high amount of lactide was converted to PLA by using catalytic extrusion with Sn(Oct)$_2$ as a cata-

lyst. Moreover, the intensity of the peak around 3400 cm$^{-1}$ in the spectra of graft co-polymer was lower than that in the spectra of pure EVOH, indicating the grafting-from by using reactive functional group (-OH group) of EVOH was generated in the catalytic extrusion. All of these results can be confirmed that the hydroxyl groups of EVOH and Sn(Oct)$_2$ are used to initiate the ring-opening polymerization of lactide by using the catalytic extrusion.
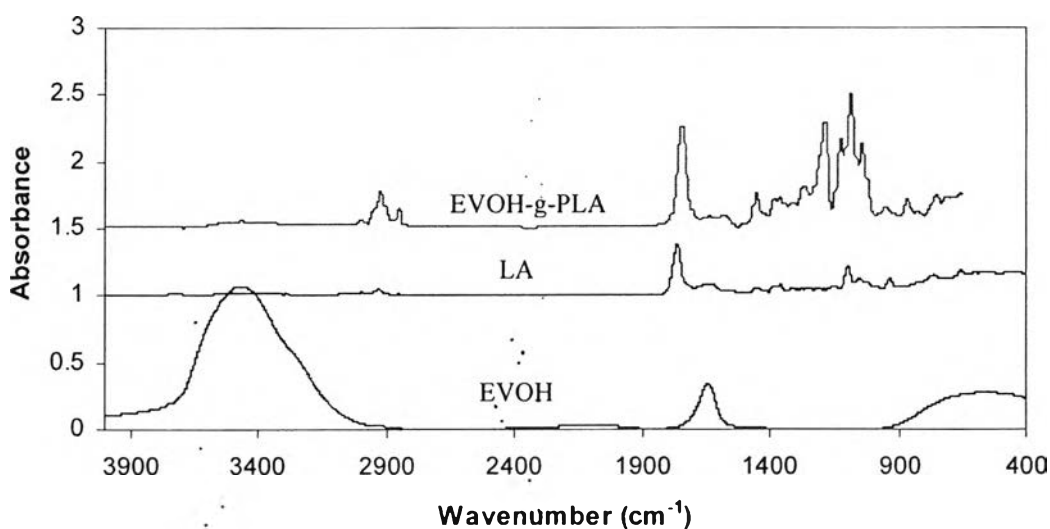


**Figure 4.8** FTIR spectra of EVOH, lactide, and isopropyl alcohol extracted EVOH-g-PLA (50/50 wt%) obtained from twin-screw extruder at 40 rpm screw speed with 0.1 wt% catalyst content.

$^1$H NMR spectra of the isopropyl alcohol extracted EVOH-g-PLA in DMSO-d$_6$ (Figure 4.9), which synthesized from 50/50 LA/EVOH content (wt%), catalyzed with 0.1 wt% Sn(Oct)$_2$ and stabilized with 5 wt% Zn/Ca stearate by using the catalytic extrusion at 40 rpm, was shown with its structure and characteristic peaks. Typical signal of PLA and EVOH components were observed. Signals at 1.2 (-CH$_3$, a), 5.15 (-CH, b), and 4.14 ppm (-OH, c) were assigned to PLA [4]. Signals at 5.0 ppm (-CH, d) and 1.2 ppm (-CH$_2$, e) assigned to EVOH backbone. Moreover, the intensity of signal at 4.05 ppm (-OH) assigned to the terminal hydroxyl group of EVOH was significantly low. This meant that the grafting reaction was generated and the degree of grafting was very high.
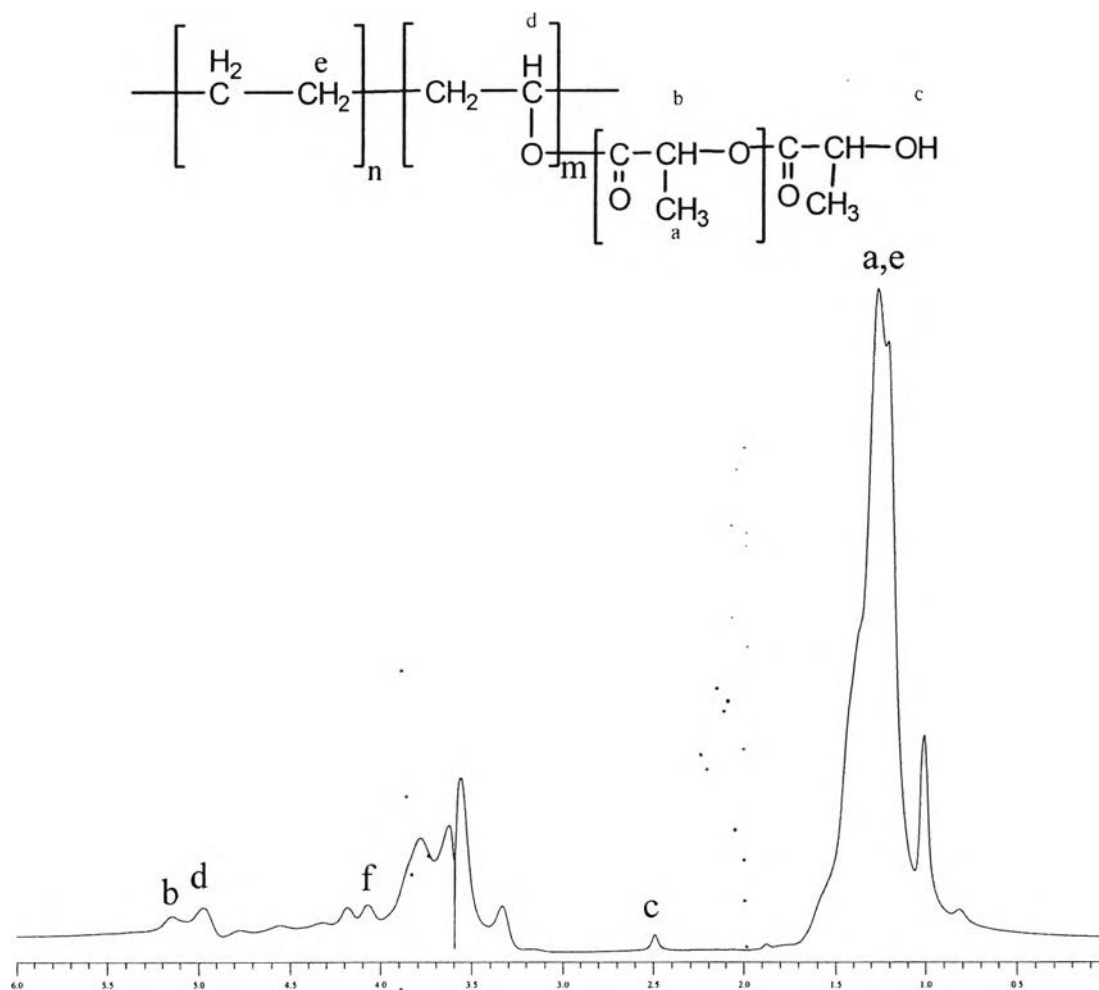
**Figure 4.9** $^1$H NMR spectra of the isopropyl alcohol extracted EVOH-g-PLA synthesized from 50/50 LA/EVOH content (wt%), catalyzed with 0.1 wt% Sn(Oct)$_2$ and stabilized with 5 wt% Zn/Ca stearate by using the catalytic extrusion at 40 rpm.

Lactide (LA) conversion was calculated from the FTIR spectrum of the cast film on KBr pellet. A calibration plot of [LA] versus $A_{935}$ was established, where $A_{935}$ is the absorptions of the bands 935 cm$^{-1}$. The absorption band at 935 cm$^{-1}$ is characteristic of LA [1]. Practically, monomer conversion (c) was calculated on the following equation:

$$c \quad = \quad 1 - ([LA]/[LA]_0) \qquad (3)$$

where

$$A_{935}/A_{1450} \quad = \quad 291.03[LA] - 0.4076 \qquad (4)$$

**Table 4.3** Lactide conversions synthesized by using a catalytic extrusion polymerization process, catalyzed with 0.1 wt% $Sn(Oct)_2$ and stabilized with 5 wt% Zn/Ca stearate

| Samples | Lactide Conversion (%) |
|:---:|:---:|
| **LA/EVOH Content (wt %)** | |
| (0.1 wt% catalyst) | |
| <u>40 rpm</u> | |
| 50/50 | 99.66 |
| 60/40 | 99.22 |
| 70/30 | 99.45 |
| 80/20 | 99.65 |
| <u>30 rpm</u> | |
| 60/40 | 99.38 |
| 70/30 | 99.56 |
| 80/20 | 99.75 |
| **Screw Speed (rpm)** | |
| (60/40 wt% LA/EVOH, 0.1 wt% catalyst) | |
| 30 | 99.38 |
| 40 | 99.22 |
| 50 | 98.96 |
| 60 | 98.65 |
| **Catalyst Content (wt%)** | |
| (60/40 wt% LA/EVOH, 30 rpm) | |
| 0.1 | 99.38 |
| 0.3 | 99.56 |
| 0.5 | 99.75 |

In table 4.3, the lactide conversion of all cases was higher than 98.7 %, shows that in all cases the ring-opening polymerization of lactide has been finished by using reactive extrusion with $Sn(Oct)_2$ as a catalyst.

Lactide conversion was shown with various LA/EVOH contents (wt%), screw speeds (rpm), and catalyst contents (wt%) in Figure 4.10. Increase in LA/EVOH contents resulted in the reduction in the lactide conversion. Due to the increase in the amount of monomer at constant catalyst content and screw speed which related to the residence time affected to the reaction time of monomer. The lactide conversion decreased with increasing screw speed because of the short time for the reaction. For the effect of the catalyst content, the reactivity of the polymerization increased with the catalyst content. Therefore, the lactide conversion increased with increasing the catalyst content.
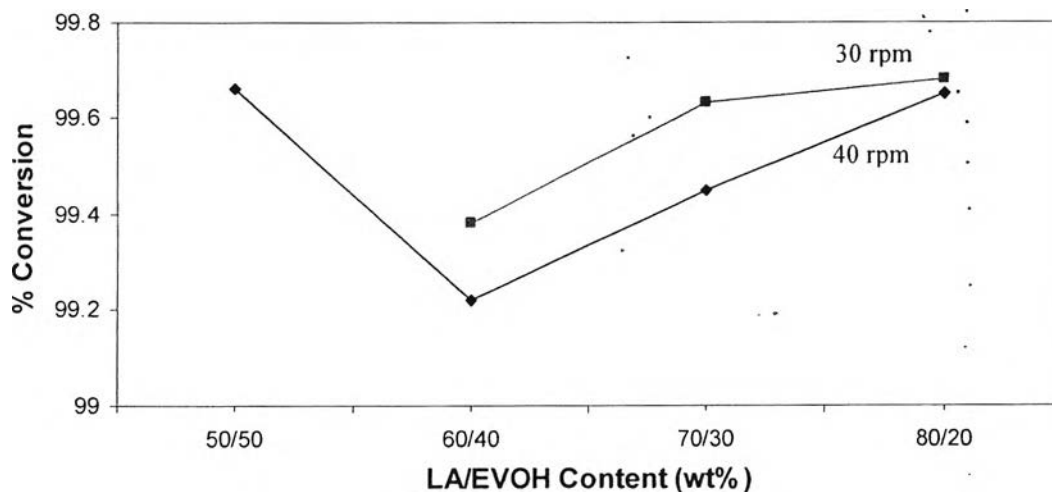


(a) 0.1 wt% $Sn(Oct)_2$ and 30 and 40 rpm screw speed
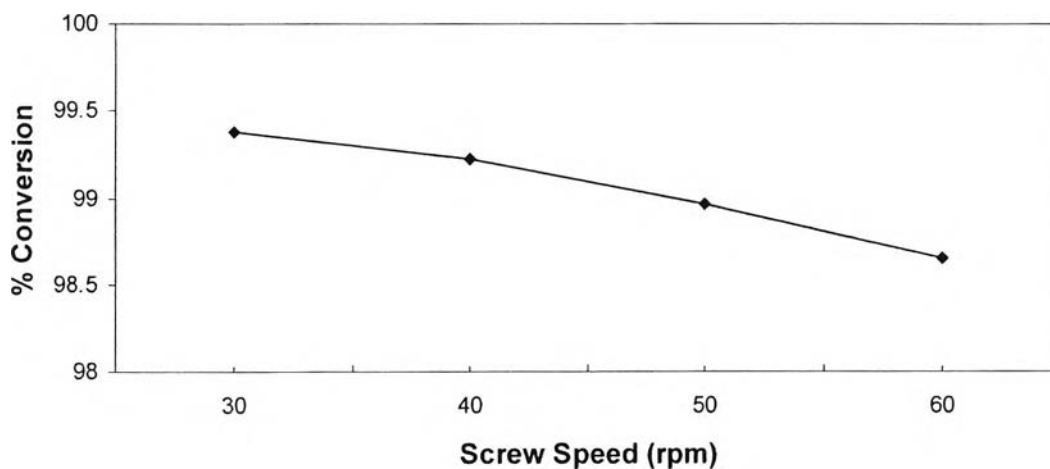
(b) 60/40 wt% LA/EVOH and 0.1 wt% Sn(Oct)$_2$
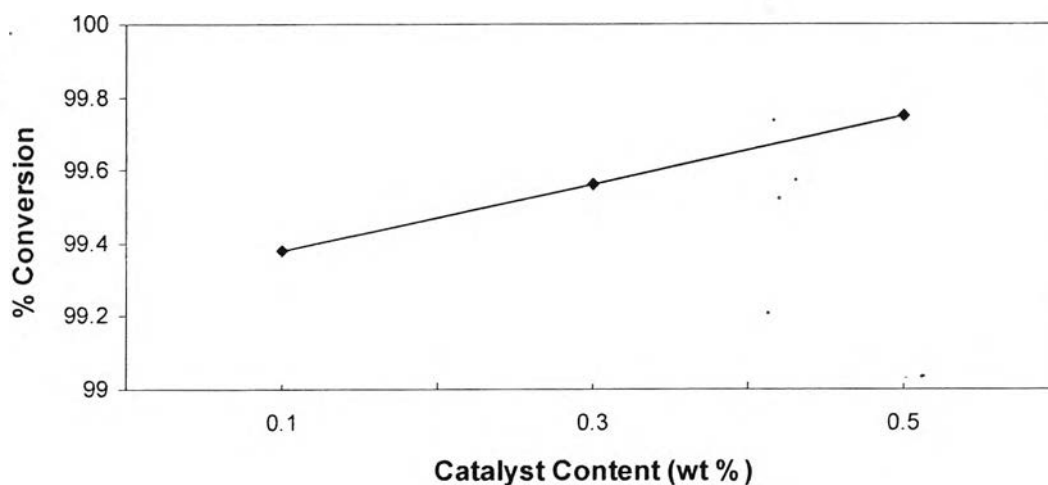


(c) 60/40 wt % LA/EVOH and 30 rpm screw speed

**Figure 4.10** Lactide conversion as the function of (a) LA/EVOH content (wt%), (b) screw speed (rpm), and (c) catalyst content (wt%).

Grafting degree (%) was calculated from the FTIR spectrum of the cast film on KBr pellet (Figures 4.11). The absorption band at 3400 cm$^{-1}$ corresponds to O-H stretching of alcohol group in EVOH. For the resulting polymers obtained from the catalytic extrusion, the concentration of O-H group in EVOH backbone was

certainly decreased compared to initial concentration. Practically, grafting degree (%) was calculated on the following equation:

$$\text{Grafting degree (\%)} = (1 - (\text{mole of OH}_r/\text{mole of OH}_i)) \times 100 \qquad (5)$$

$$A_{3400}/A_{1450} = (2 \times 10^8)(\text{mole of OH}) - 0.0454 \qquad (6)$$

where $OH_r$ was the residual O-H group after extraction with isopropyl alcohol and $OH_i$ was the initial O-H group before extraction.
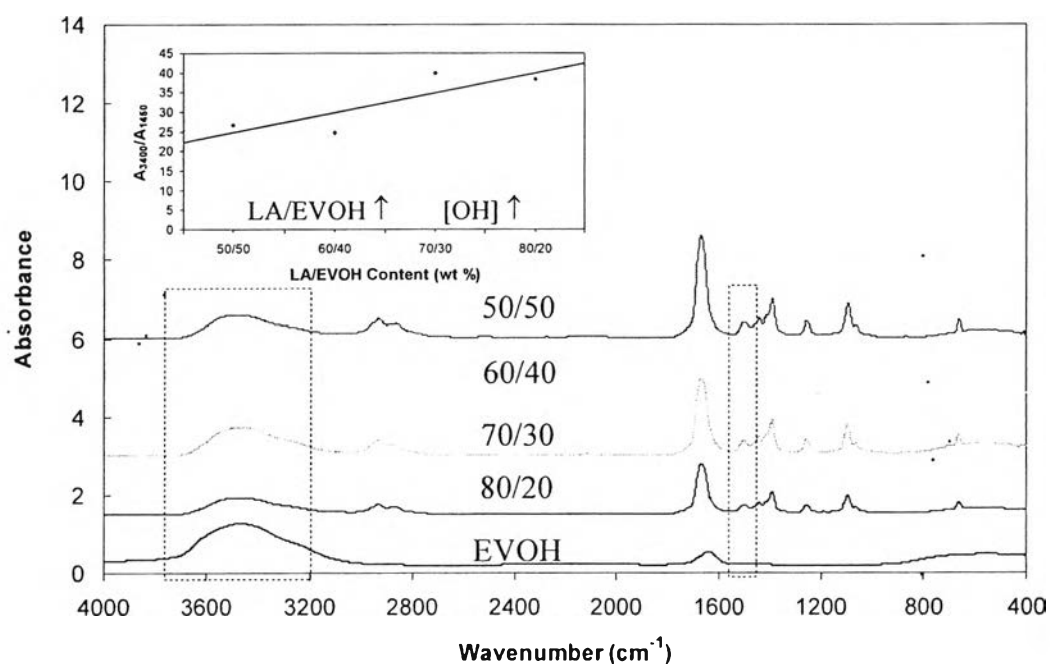


(a) 0.1 wt% Sn(Oct)$_2$ and 40 screw speed
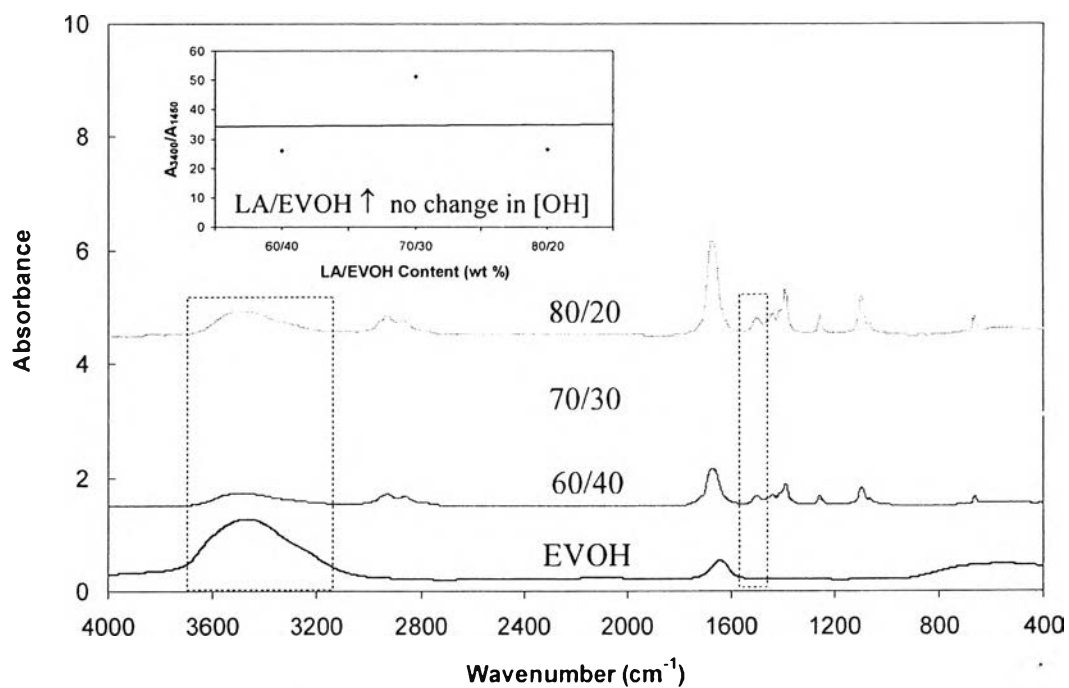
(b) 0.1 wt% Sn(Oct)$_2$ and 30 screw speed
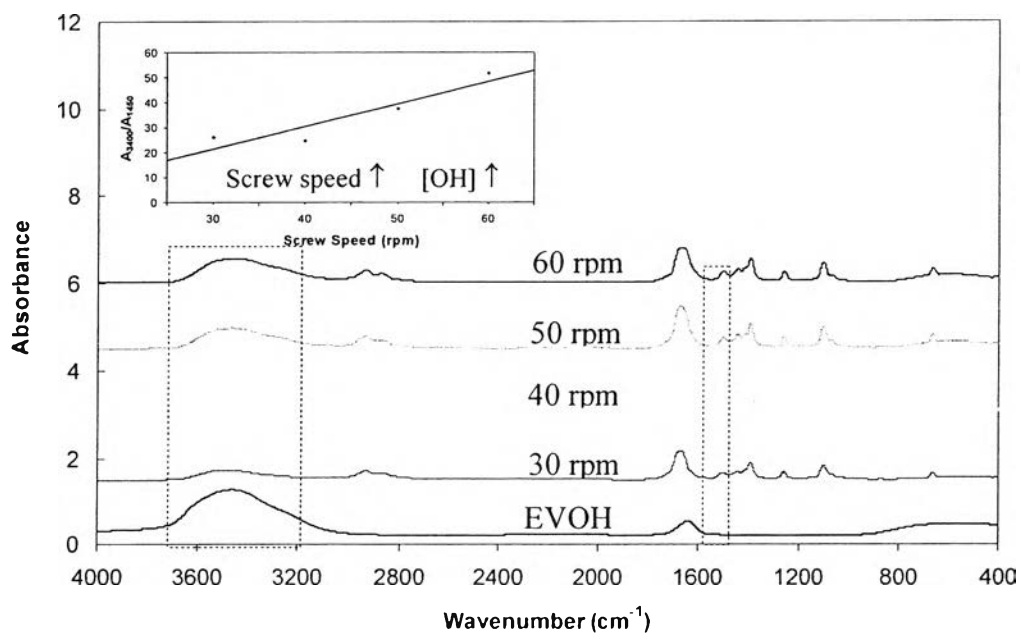


(c) 60/40 wt% LA/EVOH and 0.1 wt% Sn(Oct)$_2$
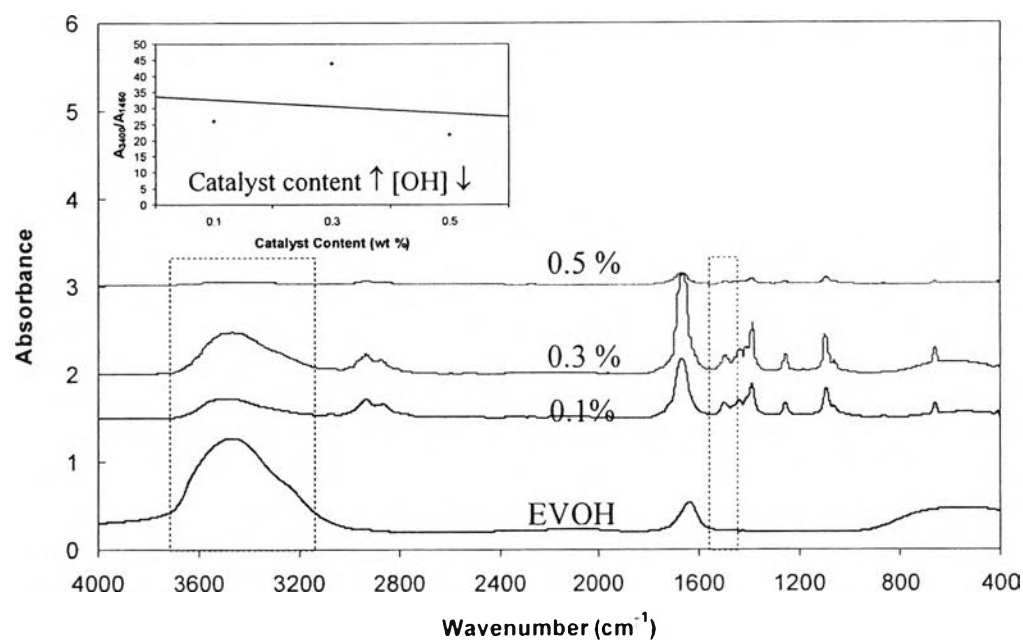
(d)·60/40 wt% LA/EVOH and 30 rpm screw speed

**Figure 4.11** FTIR spectra of EVOH and isopropyl alcohol extracted EVOH-g-PLA (Insoluble part) with varied (a) LA/EVOH content (wt%), (b) screw speed (rpm), (c) catalyst content (wt%) synthesized by using a catalytic extrusion polymerization process.

**Table 4.4** Grafting degree of extracted EVOH-g-PLA synthesized by using a catalytic extrusion polymerization process

| Samples | Grafting (%) |
|---|---|
| **LA/EVOH ratio (wt%)** | |
| (60/40 wt% LA/EVOH, 0.1 wt% catalyst) | |
| <u>40 rpm</u> | |
| 50/50 | 84.70 |
| 60/40 | 82.31 |
| 70/30 | 61.85 |
| 80/20 | 45.17 |

| 30 rpm | |
|---|---|
| 60/40 | 81.40 |
| 70/30 | 51.13 |
| 80/20 | 62.12 |
| **Screw Speed (rpm)** | |
| (0.1 wt% catalyst) | |
| 30 | 81.40 |
| 40 | 82.31 |
| 50 | 73.16 |
| 60 | 63.15 |
| **Catalyst Content (wt%)** | |
| (60/40 wt % LA/EVOH, 30 rpm) | |
| 0.1 | 81.40 |
| 0.3 | 81.16 |
| 0.5 | 84.44 |

In Table 4.4, the influence of LA/EVOH content, the extruder screw speed, and catalyst content on the grafting degree is shown. According to the grafting degree of the copolymers with varied LA/EVOH content, it showed that the grafting degree dropped with increasing the LA/EVOH content. The screw speed was varied between 30, 40, 50, and 60 rpm and 60/40 LA/EVOH content (wt%) has been used. Raising the screw speed from 30 to 60 rpm reduced the degree of grafting. The reason for this behavior is, as the remaining residence time inside the twin-screw extruder decreased with increasing screw speed, which resulted in a grafting reaction not finished at the extruder die. Therefore, the optimum screw speed was 40 rpm for this case. Finally, varying the catalyst content, the grafting degrees were in the same level. This meant that the catalyst content did not significantly affect to the grafting degree of graft copolymer.

### 4.4.7 Molecular weight measurement

Molecular weight and molecular weight distribution of the resulting polymers was measured by using the gel permeation chromatography (GPC). GPC was carried out in DMF using a DMF column with a reflactometer index detector. Molecular weight and molecular weight distribution of these polymers were calculated in reference to a following polystyrene calibration:
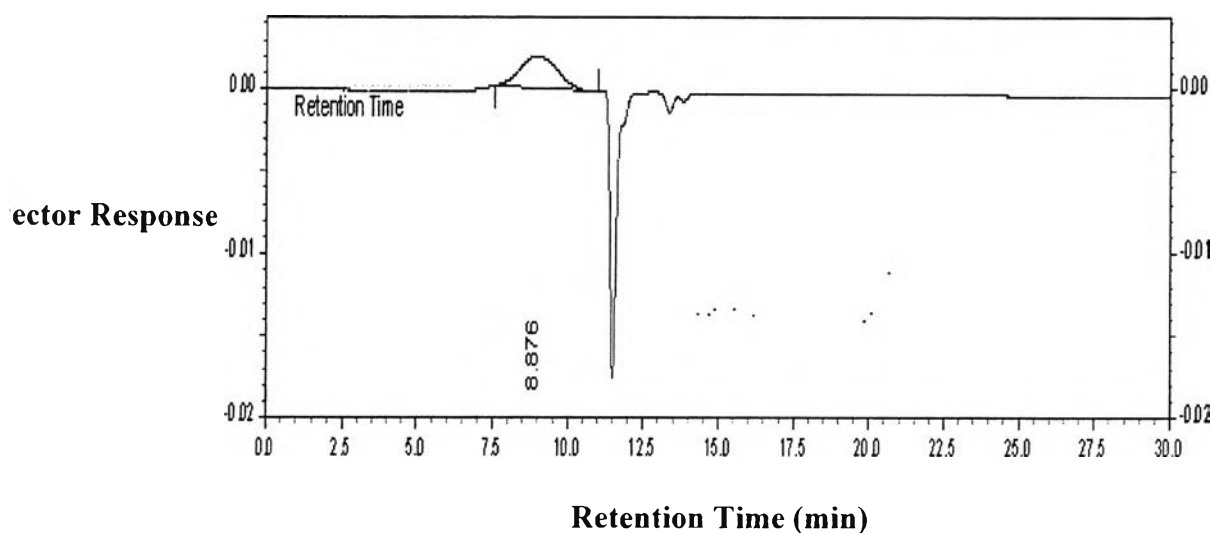
$$\log M = -0.85277955t + 13.00123578 \qquad (7)$$
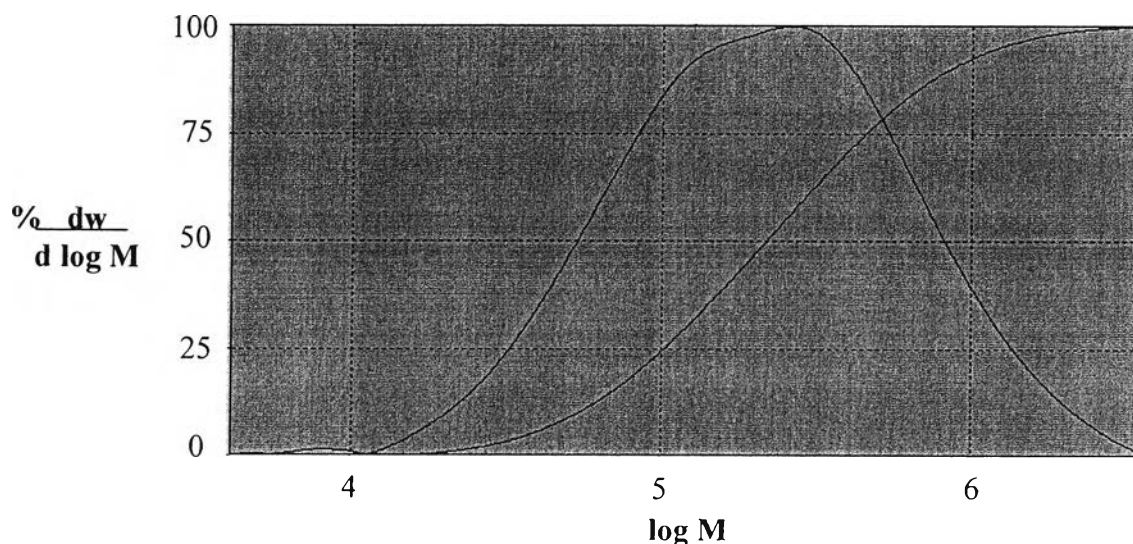


**Figure 4.12** GPC curve for isopropyl alcohol extracted EVOH-g-PLA with 70/30 wt% LA/EVOH content, 0.1 wt% Sn(Oct)$_2$, 5 wt% Zn/Ca stearate, and 30 rpm screw speed.

**Table 4.5** Molecular weight and molecular weight distribution of isopropyl alcohol extracted EVOH-g-PLA synthesized by using a catalytic extrusion polymerization process

| Samples | $M_w \times 10^4$ (g/mol) | $M_n \times 10^4$ (g/mol) | $M_w/M_n$ |
|---|---|---|---|
| Commercial PLA | 9.11 | 16.4 | 1.8 |
| Commercial EVOH | 10.7 | 5.7 | 1.9 |
| **LA/EVOH Content (wt%)** | | | |
| 40 rpm | | | |
| 50/50 | 36.6 | 36.2 | 1.0 |
| 60/40 | 32.0 | 16.0 | 2.0 |
| 70/30 | 29.5 | 16.0 | 1.8 |
| 80/20 | 24.8 | 12.9 | 1.9 |
| 30 rpm | | | |
| 60/40 | 27.8 | 14.4 | 1.9 |
| 70/30 | 24.5 | 14.4 | 1.7 |
| 80/20 | 28.4 | 15.4 | 1.8 |
| **Screw Speed (rpm)** | | | |
| 30 | 27.8 | 14.4 | 1.9 |
| 40 | 32.0 | 16.0 | 2.0 |
| 50 | 27.4 | 14.8 | 1.9 |
| 60 | 27.5 | 18.1 | 1.5 |
| **Catalyst Content (wt%)** | | | |
| 0.1 | 27.8 | 14.4 | 1.9 |
| 0.3 | 31.0 | 16.5 | 1.9 |
| 0.5 | 29.0 | 15.4 | 1.9 |

Weight average molecular weight ($M_w$), molecular weight distribution (MWD), and degree of grafting as a function of LA/EVOH content are shown in Figure 4.13 (a) and (b). Raising in the LA/EVOH content from 50/50 to 80/20 wt% decreased the degree of grafting at the same 40 rpm screw speed. In Figure 4.13 (a), it meant that 40 rpm screw speed did not give enough residence time for high monomer content. For the experiment carried out at fixed 30 rpm, the grafting degree with increasing the LA/EVOH content which was the same as the case of 40 rpm. However, in this case, it was clearly seen that the weight average molecular weight decreased as a function of LA/EVOH content. Moreover, the molecular weight distribution was smaller than 2. This showed that the degradation reaction or chain scission have been very limited, which is due to the use of Ca/Zn stearate as stabilizing agent.

A set of experiment was used to determine the influence of the extruder screw speed on the resulting polymer parameters (Figure 4.14). This experiment was carried out using 60/40 wt% LA/EVOH content. The screw speed was varied between 30, 40, 50, and 60 rpm. Raising the screw speed reduced the degree of grafting. For the effect of the screw speed on the molecular weight and the molecular weight distribution, two main influences can be described. First, increasing screw speed leads to reduced residence time, which in turn should reduce the molecular weight and enhanced the molecular weight distribution. Second, the higher screw speed increased the degree of mixing and the shear introduction into the melt, which in turn increased the rate of reaction, favoring degradation and side reactions to enhance the molecular weight distribution [1]. In this case, the fusion behavior of products obtained from brabender mixer particularly in the case of 205 °C rotor temperature suggested that the effect of residence time is more significant than the effect of shearing. The reaction of 50/50 wt% LA/EVOH content operated at 40 rpm rotor speed started after 6 min (Figure 4.15 (a)), whereas the reaction operated at 60 rpm rotor speed started after 18 min (Figure 4.15 (b)). This showed that the case of 60 rpm rotor speed, which generated larger torque and introduced higher shear in comparison with 40 rpm rotor speed, used longer time to succeed the reaction. In addition, the temperature was not significantly increased with time due to no change in viscosity of the melt.

In Figure 4.15, the catalyst concentration increased the degree of grafting due to high concentration of catalyst can improve the reactivity of the reaction. For the molecular weight of the resulting polymers, the catalyst concentration about 0.3 wt% gave the highest molecular weight. Even though, the molecular weight of the resulting polymer catalyzed with 0.3 wt% stannous octoate was not much higher than that of the resulting polymer catalyzed with 0.1 wt% stannous octoate. Therefore, the catalyst concentration about 0.1 wt% was enough for this case.
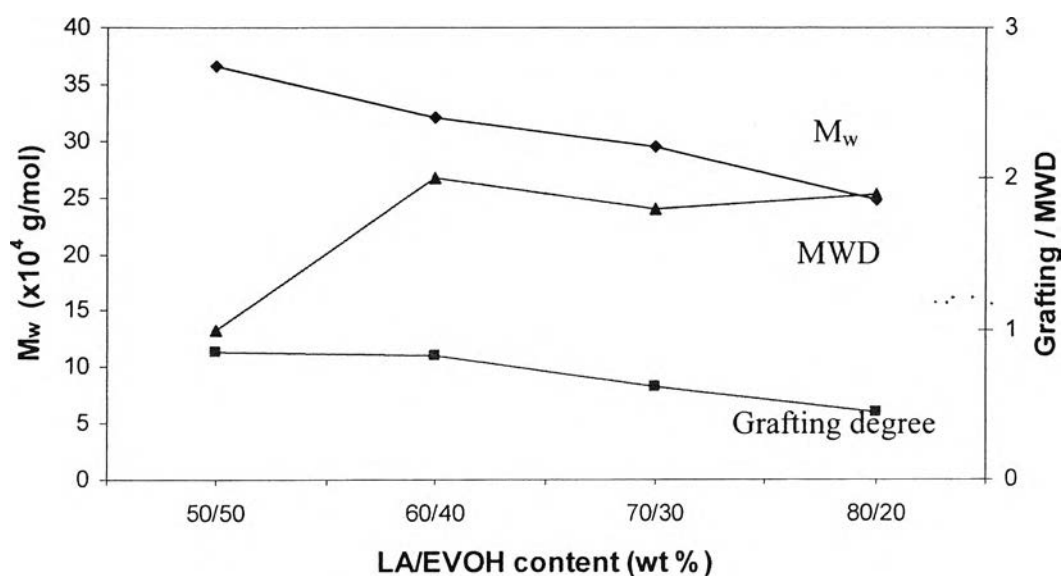


(a)
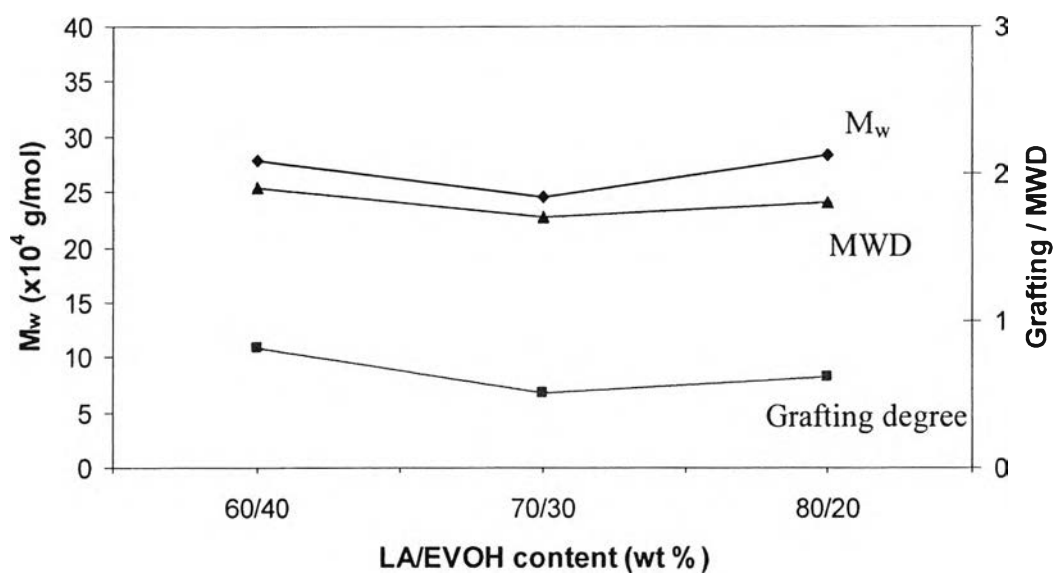
(b)

**Figure 4.13** Molecular parameters of isopropyl alcohol extracted EVOH-g-PLA received in reactive extrusion polymerization with 60/40 wt% LA/EVOH, 0.1 wt% Sn(Oct)$_2$, and 5 wt% Zn/Ca stearate in dependence of LA/EVOH content at (a) 40 rpm and (b) 30 rpm screw speed.
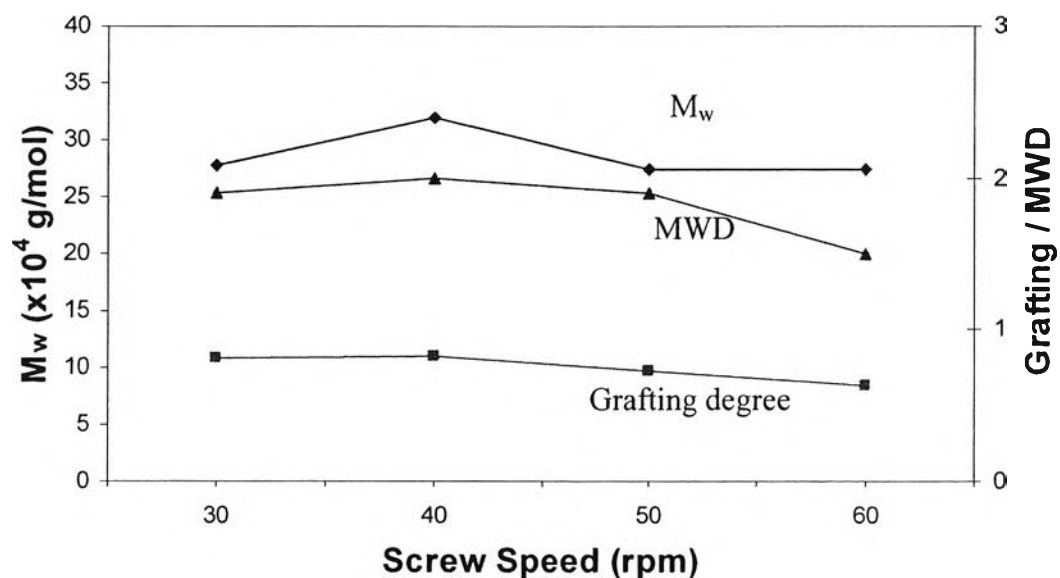
**Figure 4.14** Molecular parameters of isopropyl alcohol extracted EVOH-g-PLA received in reactive extrusion polymerization with 60/40 wt% LA/EVOH, 0.1 wt% $Sn(Oct)_2$, and 5 wt% Zn/Ca stearate in dependence of the screw speed.
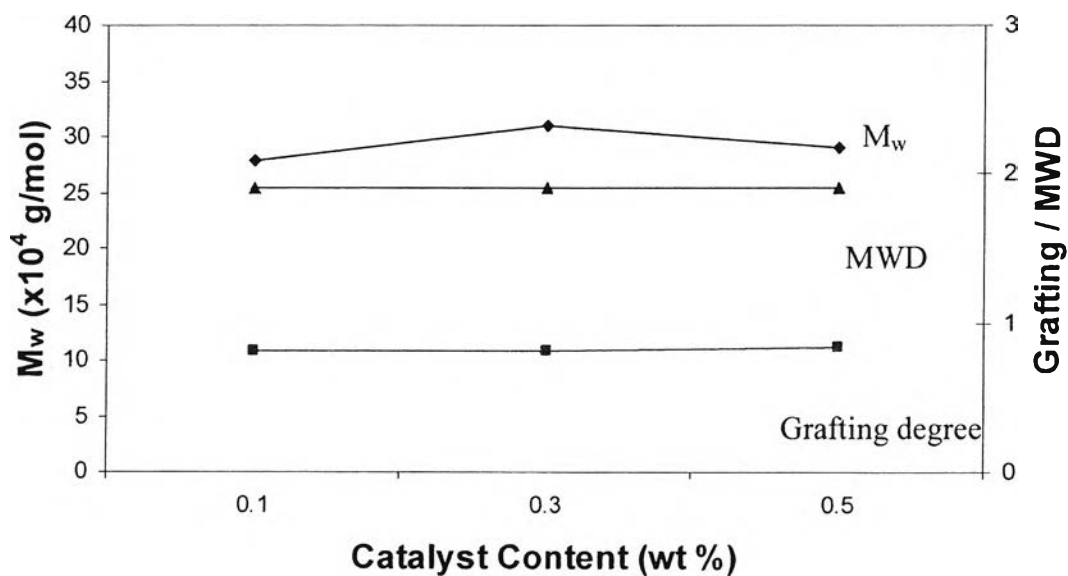


**Figure 4.15** Molecular parameters of extracted EVOH-g-PLA received in reactive extrusion polymerization with 60/40 wt% LA/EVOH, 30 rpm screw speed, and 5 wt% Zn/Ca stearate in dependence of the catalyst content.

### 4.4.8 Thermal analysis

To determine the thermal behavior of the graft copolymers DSC measurements have been carried out. Results of crude EVOH-g-PLA produced in a reactive extrusion polymerization are shown in Figure 4.16. The samples have been heated to 200 °C and cooled to 30 °C. Following this, they were heated from 30 °C to 200 °C with a constant heating rate of 10 K/min. The glass-transition temperature of graft copolymers was lower than that of pure EVOH, indicating the decrease in rigidity. Moreover the curves displayed only glass transition. The melting peaks were not observed. This shows that the grafting obstructed the crystallization.
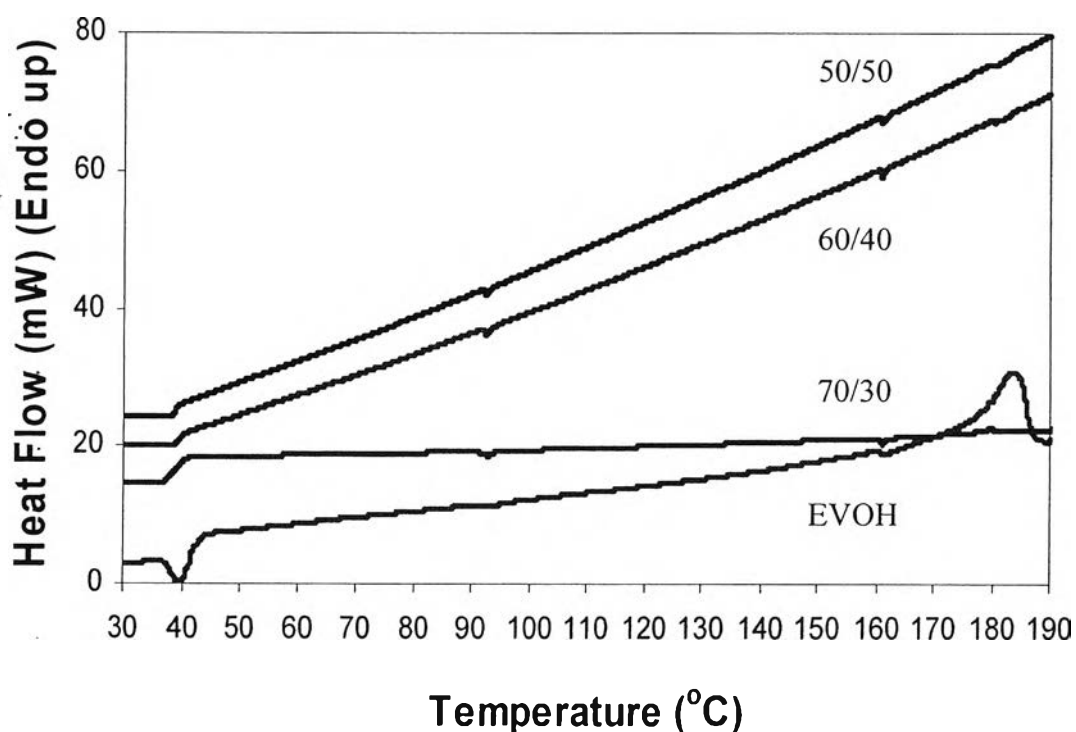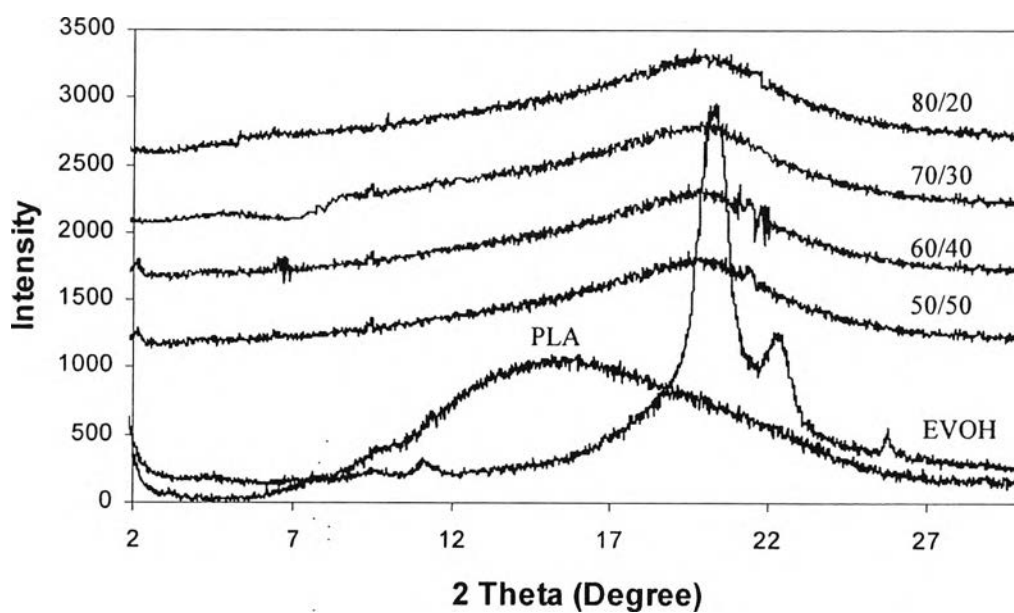


**Figure 4.16** DSC-measurement of crude EVOH-g-PLA produced in reactive extrusion polymerization with 0.1 wt% Sn(Oct)$_2$, 5 wt% Zn/Ca stearate, and 40 rpm screw speed in dependence of LA/EVOH content. First heating and cooling at 10 K/min heating rates.
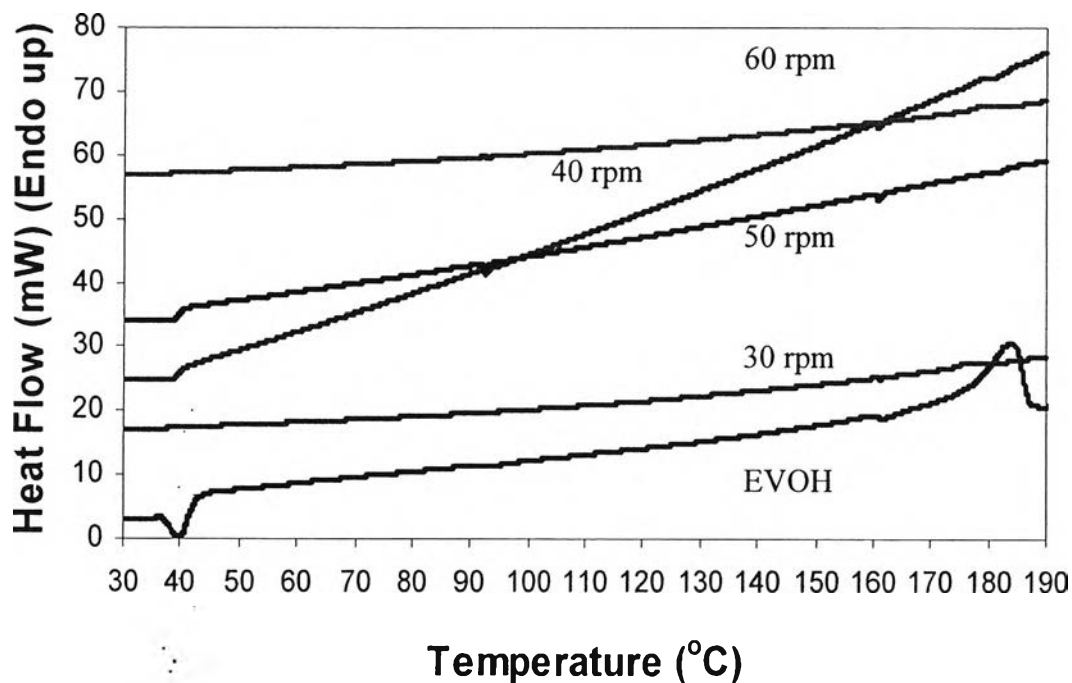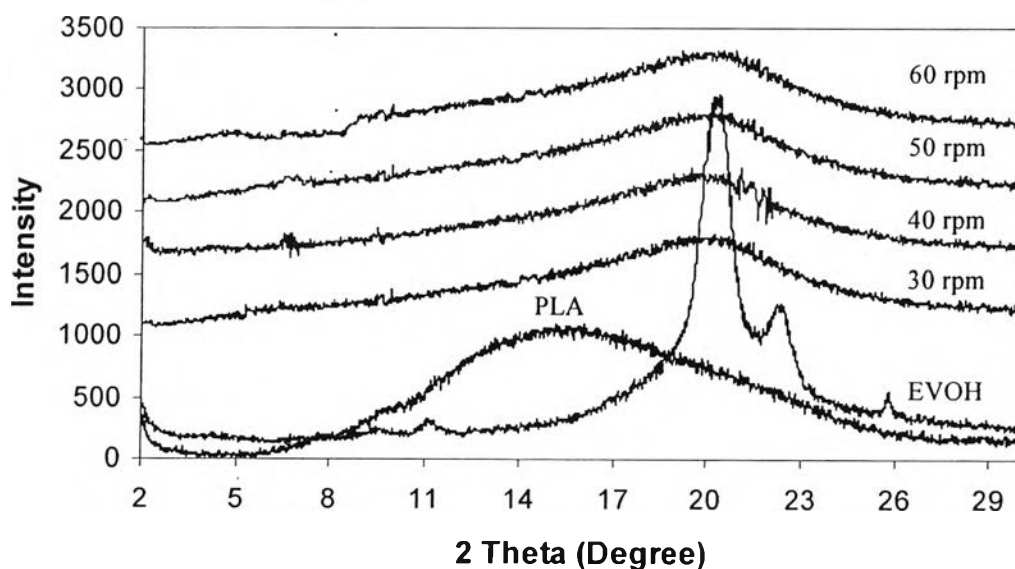
**Figure 4.17** DSC-measurement of crude EVOH-g-PLA produced in reactive extrusion polymerization with 60/40 wt% LA/EVOH content, 0.1 wt% $Sn(Oct)_2$, and 5 wt% Zn/Ca stearate in dependence of screw speed. First heating and cooling at 10 K/min heating rates.

The results of XRD (Figure 4.18 and 4.19) confirm the thermal and crystallization behavior of graft copolymer. Pure PLA exhibits a broad crystalline peak at 16.6° 2θ, whereas pure EVOH exhibits a very strong crystalline peak at 20.5° 2θ. For the curves of graft copolymer, they had the same peak positions at 20° 2θ and all of the peaks were short and broad. The comparison of X-ray diffraction profile of pure PLA, pure EVOH, and graft copolymers indicated that the grafting had destroyed the original crystallization of pure PLA and changed the original molecular structure of pure EVOH.

**Figure 4.18** XRD patterns of crude EVOH-g-PLA produced in reactive extrusion polymerization with 0.1 wt% Sn(Oct)$_2$, 5 wt% Zn/Ca stearate, and 40 rpm screw speed in dependence of LA/EVOH content.



**Figure 4.19** XRD patterns of crude EVOH-g-PLA produced in reactive extrusion polymerization with 60/40 wt% LA/EVOH content, 0.1 wt% Sn(Oct)$_2$, and 5 wt% Zn/Ca stearate in dependence of screw speed.

The TG-DTA curves of crude EVOH-g-PLA are shown in Figures 4.20, 4.21, and 4.22 and some results of thermal properties are listed in Table 4.6. From TGA curve, it could be seen that 2-6 % weight loss in the temperature range of 50-200 °C is due to the evaporation of absorbed water and loss of some products on the surface and in the temperature range of 500-550°C, the loss of the stabilizer caused about 10 % weight loss. Moreover, for the resulting polymers, there were two main mass loss steps, the first step due to the weight loss of PLA component, which was the major component, was observed at the temperature range of 241-278 °C. The other step was attributed to EVOH component, which was the minor component, from 408-419 °C. Compared to the curves of pure polymers, the thermal decomposition temperature of PLA and EVOH was 327.1 and 341.0/425 °C, respectively. All graft copolymers showed that the thermal decomposition temperatures of the PLA component appear to be lower when compared to the pure PLA and the thermal decomposition temperatures of the EVOH component appear to remain only high temperature component (ethylene component) compared to the pure EVOH. This could be indicated that the thermal degradation efficiency of the resulting polymers polymerized by using the catalytic extrusion was significantly increased when compared to origin PLA. The lowering of PLA in EVOH-g-PLA decomposition is attributed to amorphous nature. Due to PLA grafted from EVOH significantly suppressed the crystallization of the EVOH moiety [27], the degradation temperature of PLA component in graft copolymer decreased. In contrast to the plasticized PLA, the plasticizer made crystallization of PLA more easy and complete [28], so the degradation temperature of plasticized PLA is higher than that of pure PLA. However, thermal stability is better for the blend with higher molecular weight. On the other hand, decomposition temperature of EVOH is shifted to higher temperature indicating less vinyl alcohol is presented and so confirm the success of grafting-from via catalytic extrusion.
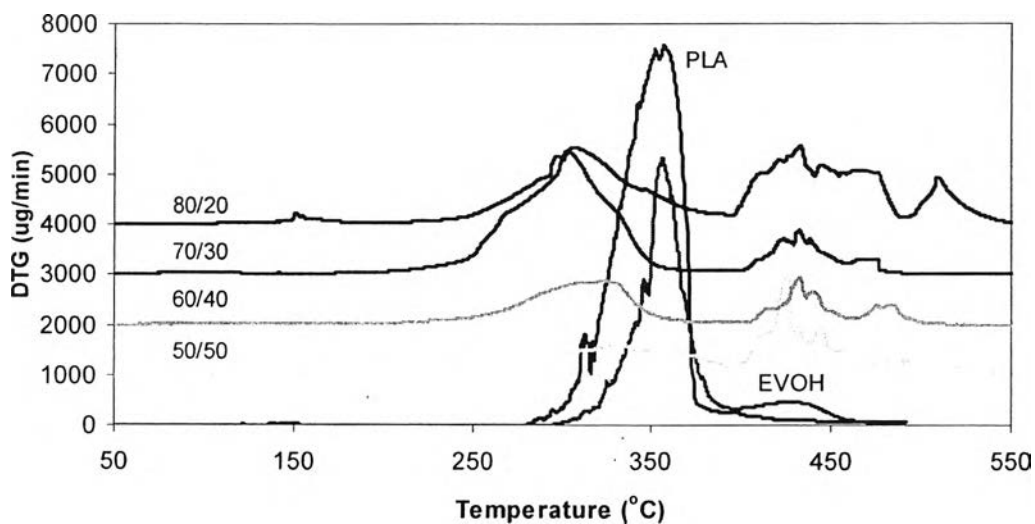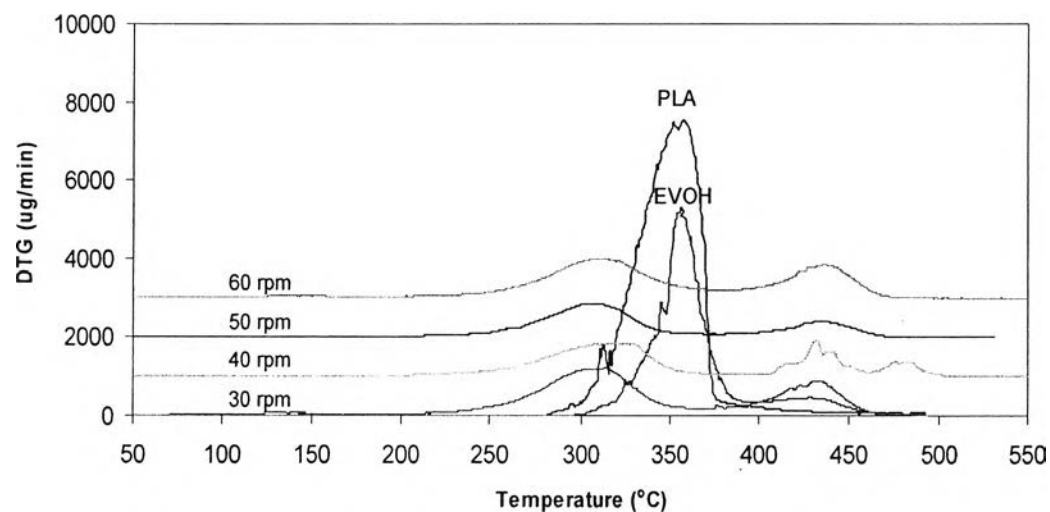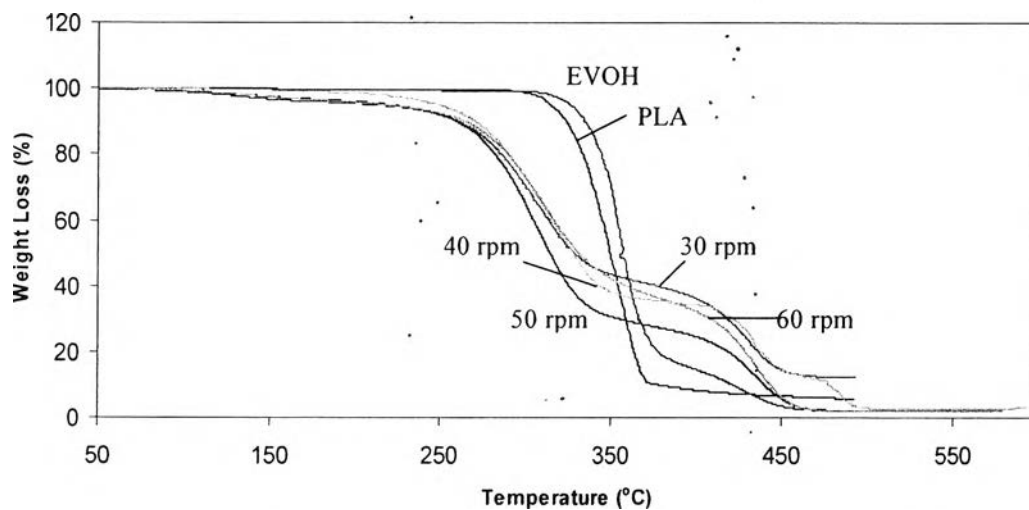
(a)
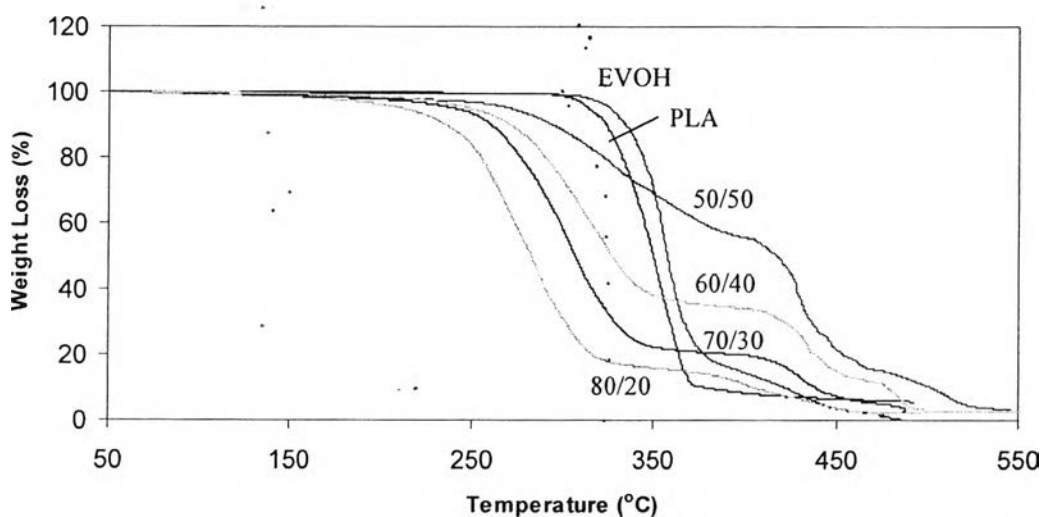


(b)

**Figure 4.20** TG-DTA curve of crude EVOH-g-PLA synthesized by using a catalytic extrusion polymerization process with 40 rpm screw speed, catalyzed with 0.1 wt% Sn(Oct)$_2$ and stabilized with 5 wt% Zn/Ca stearate, with the varied the monomer to polymer ratio (a) differential weight loss curves (DTG) (b) weight losses of the samples.
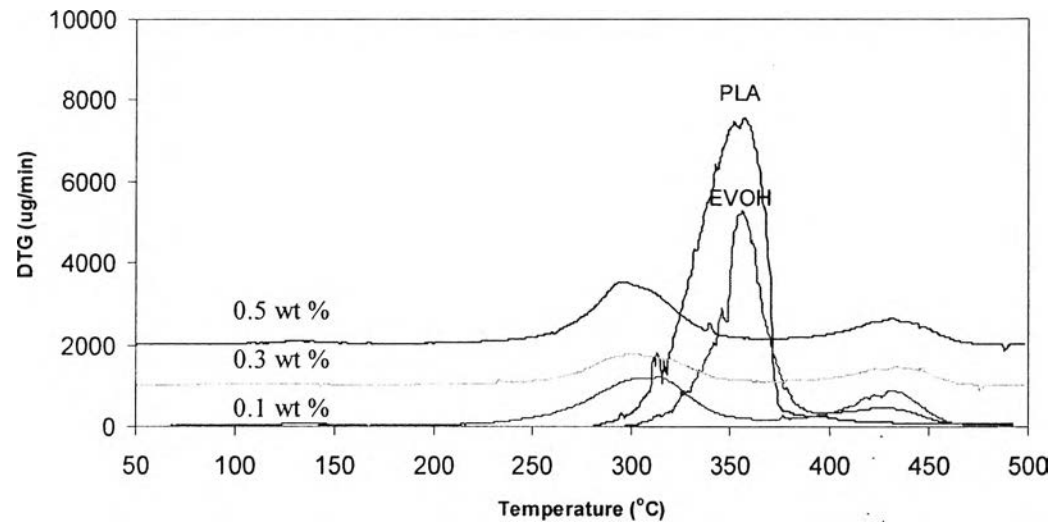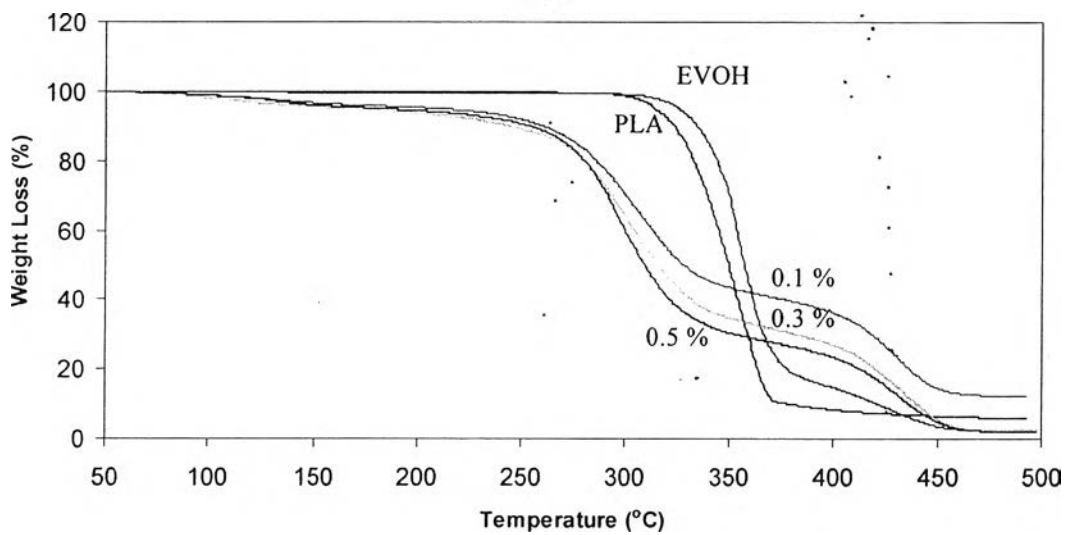
(a)



(b)

**Figure 4.21** TG-DTA curve of crude EVOH-g-PLA synthesized by using a catalytic extrusion polymerization process with 60/40 LA/EVOH ratio, catalyzed with 0.1 wt% Sn(Oct)$_2$ and stabilized with 5 wt% Zn/Ca stearate, with the varied screw speed (a) differential weight loss curves (DTG) (b) weight losses of the samples.

(a)



(b)

**Figure 4.22** TG-DTA curve of crude EVOH-g-PLA synthesized by using a catalytic extrusion polymerization process with 60/40 LA/EVOH ratio and 30 rpm screw speed, catalyzed with 0.1 wt% Sn(Oct)$_2$ and stabilized with 5 wt% Zn/Ca stearate, with the varied catalyst content (a) differential weight loss curves (DTG) (b) weight losses of the samples.

**Table 4.6** Thermal properties of crude EVOH-g-PLA synthesized by using a catalytic extrusion polymerization process

| Samples | $T_d$ onset (°C) | | Weight Loss (%) | | | Char Residual (wt %) |
|---|---|---|---|---|---|---|
| | PLA | EVOH | H₂O | PLA | EVOH | |
| Commercial PLA | 327.1 | - | - | 93.1 | - | 6.9 |
| Commercial EVOH | - | 341.0 | 2.8 | - | 83.9 | 13.3 |
| **LA/EVOH Content (wt%)** | | | | | | |
| 50/50 | 278.7 | 420.7 | 2.0 | 45.0 | 41.0 | 12.0 |
| 60/40 | 274.8 | 419.0 | 1.5 | 65.0 | 21.5 | 12.0 |
| 70/30 | 265.4 | 415.0 | 2.0 | 78.2 | 14.8 | 5.0 |
| 80/20 | 241.0 | 408.0 | 4.0 | 79.0 | 15.0 | 2.0 |
| **Screw Speed (rpm)** | | | | | | |
| 30 | 267.3 | 410.3 | 5.5 | 50.5 | 42.7 | 1.3 |
| 40 | 274.8 | 419.0 | 1.5 | 65.0 | 21.5 | 12.0 |
| 50 | 273.0 | 414.6 | 3.8 | 66.9 | 26.7 | 2.6 |
| 60 | 275.0 | 415.2 | 1.4 | 58.6 | 35.9 | 2.1 |
| **Catalyst Content (wt%)** | | | | | | |
| 0.1 | 276.0 | 411.9 | 5.5 | 50.5 | 42.7 | 1.3 |
| 0.3 | 269.8 | 410.4 | 5.0 | 62.3 | 29.9 | 2.8 |
| 0.5 | 272.3 | 408.5 | 6.0 | 67.1 | 25.2 | 1.7 |

### 4.4.7 Dynamic-mechanical analysis

The DMA results for the crude graft copolymers with various LA/EVOH contents are presented in Figures 4.23, 4.24, and 4.25. The glass-transition temperature taken at the maximum of tan δ peaks increased with increasing LA/EVOH contents because the amount of PLA homopolymer increased with increased in LA/EVOH content. These results in Figure 4.23 (a) are clearly seen that the glass-transition temperature of all graft copolymers, which is around 26.7, 30.5, 11.5, and 44.0 °C for 50/50, 60/40, 70/30, and 80/20 wt% LA/EVOH contents re-

spectively, was significant lower than 80 °C of pure PLA, indicating enhance in the mobility and the reduction in the rigidity.

In Figures 4.23 (b) and (c) show the storage modulus (E') and the loss modulus (E'') of graft copolymers as the function of temperature. For pure PLA, the storage modulus dropped drastically between 65 °C and 90 °C which was its glass-transition region. Whereas, the storage modulus of graft copolymers gradually decreased between -10 °C and 80 °C accompanied the broad dispersion of tan δ peaks. The modulus drop of about two orders of magnitude accorded with pure PLA. Whereas, the graft copolymers showed the modulus drop of about five orders of magnitude.

The tan δ of graft copolymers with different screw speeds is shown in the Figure 4.24 (a). The glass-transition temperature of graft copolymers with varied 30, 40, 50, and 60 rpm screw speed exhibits in the same level around 35 °C. Therefore, it can be concluded that the glass-transition temperature of graft copolymer did not depend on the screw speed. In addition, the catalyst content affected to the tan δ. The glass-transition of graft copolymers with various catalyst contents were equal in the case of 0.1 and 0.5 wt% but in the case of 0.3 wt%, it showed the higher glass-transition temperature (Figure 4.25 (a)). Moreover, all curves of tan δ reveal these blends are miscible.
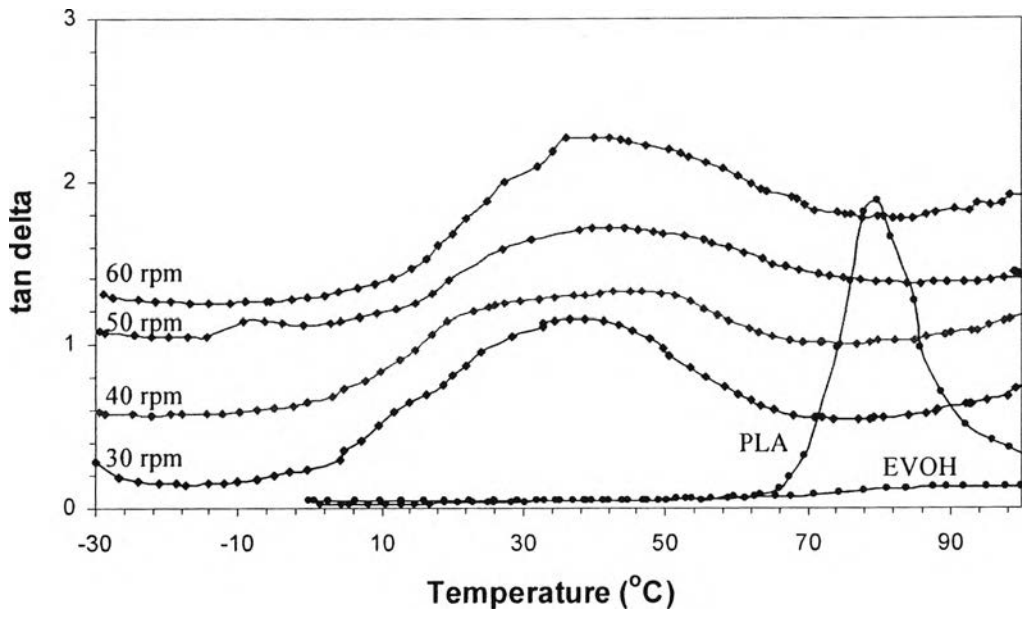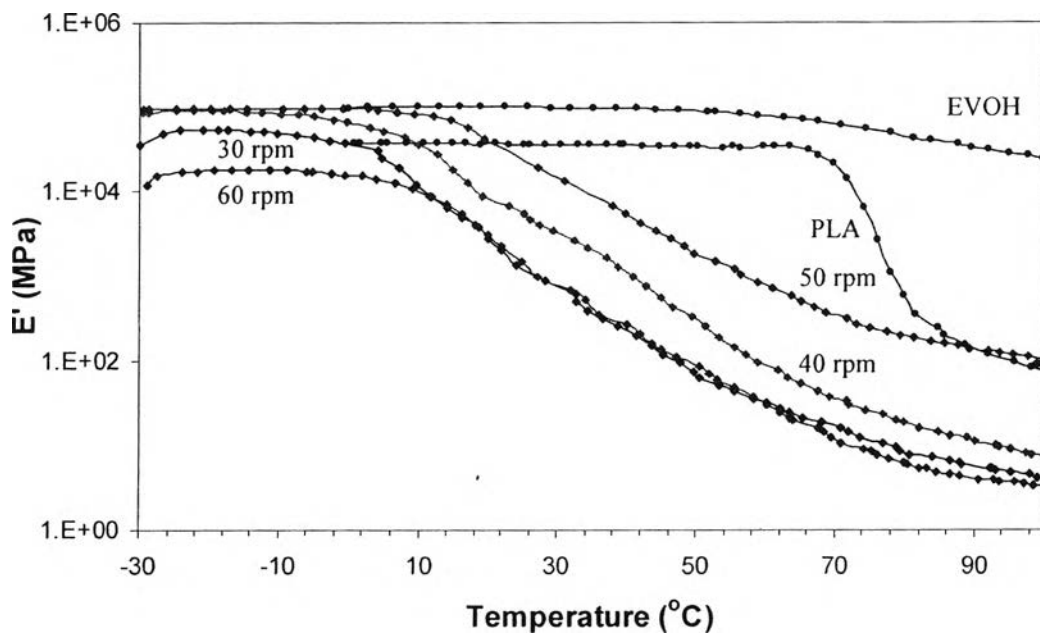
(a)



(b)
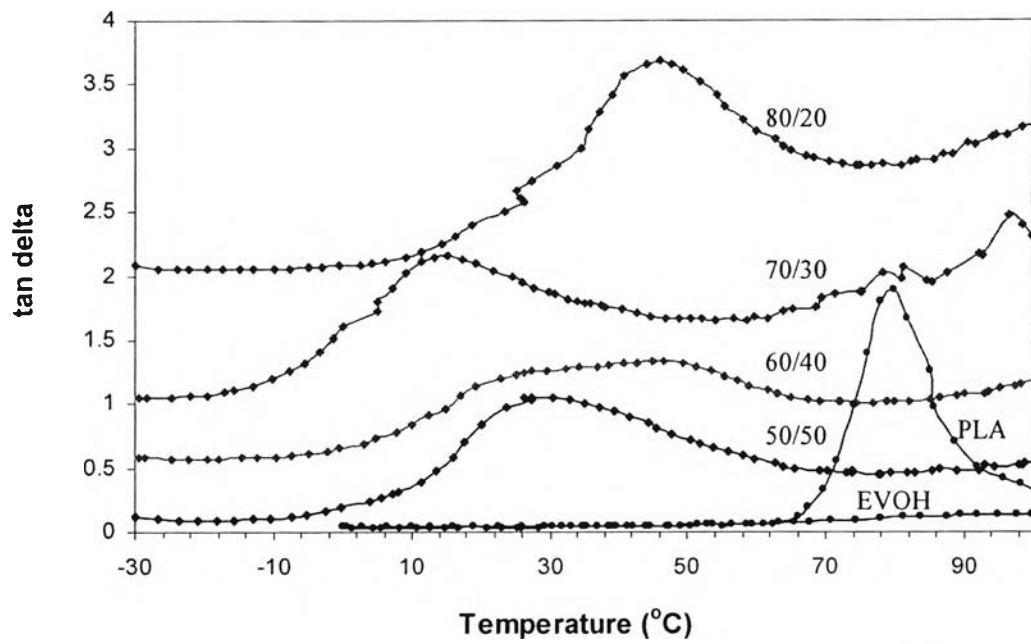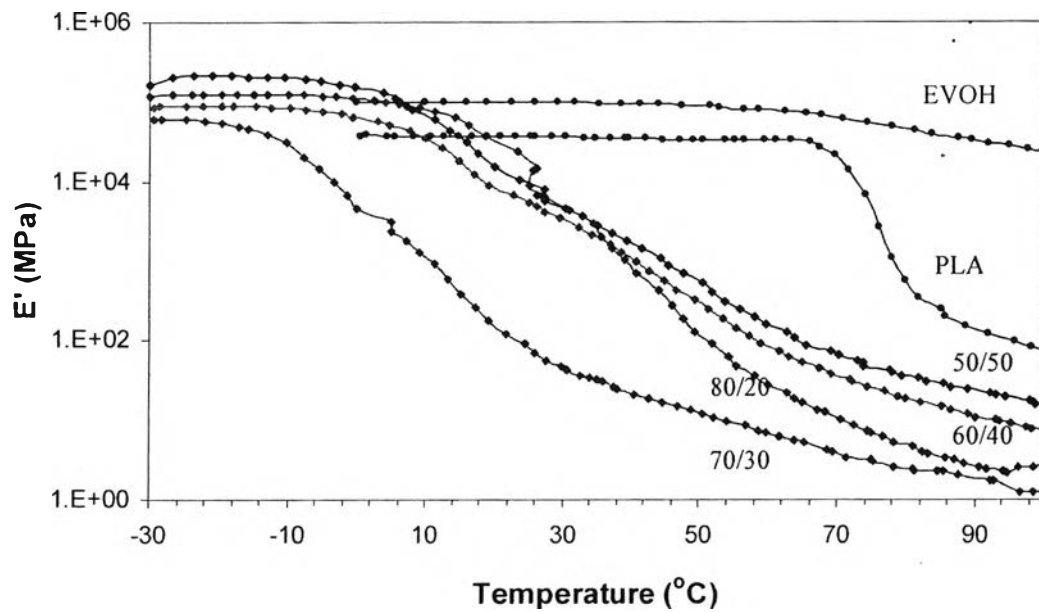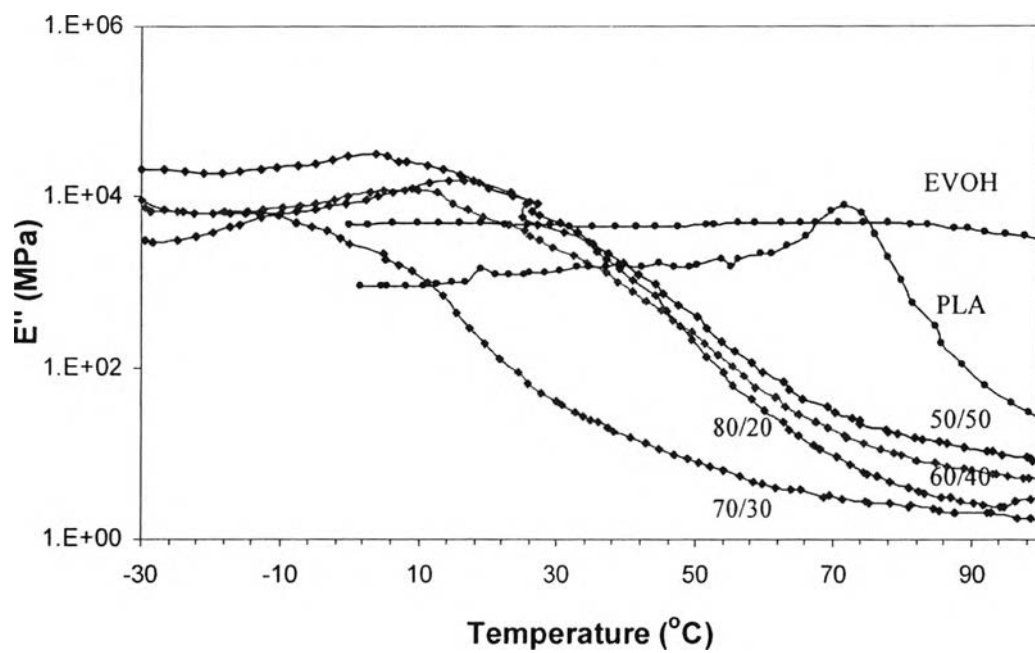
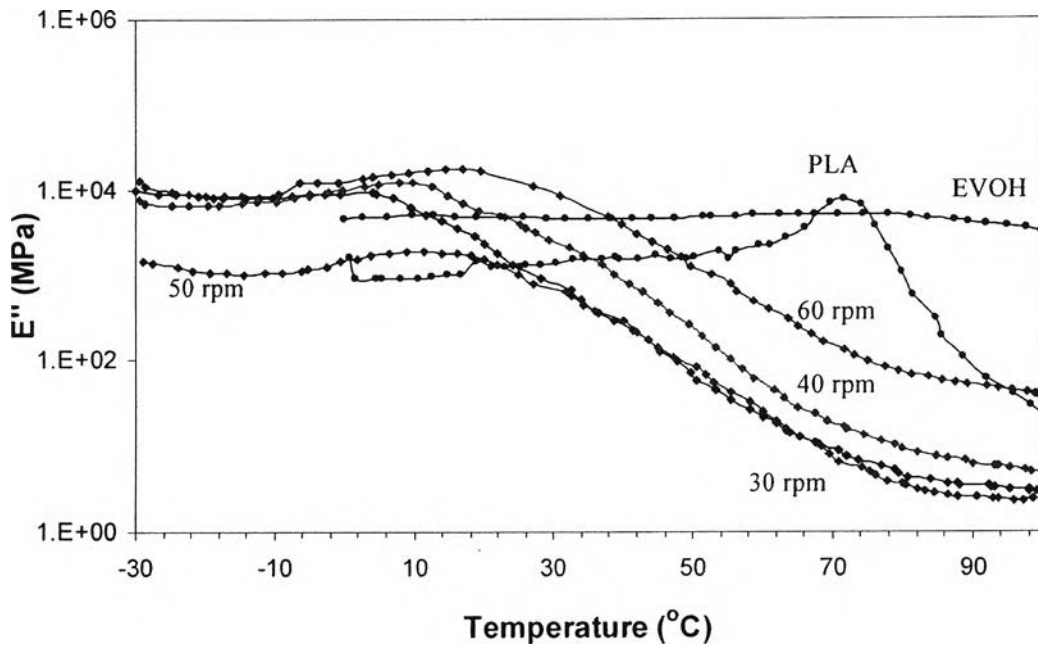Figure 4.23 DMA results of crude EVOH-g-PLA produced in reactive extrusion polymerization with 0.1 wt% Sn(Oct)$_2$, 5 wt% Zn/Ca stearate, and 40 rpm screw speed in dependence of LA/EVOH content (a) tan $\delta$, (b) E', and (c) E'' as the function of temperature.
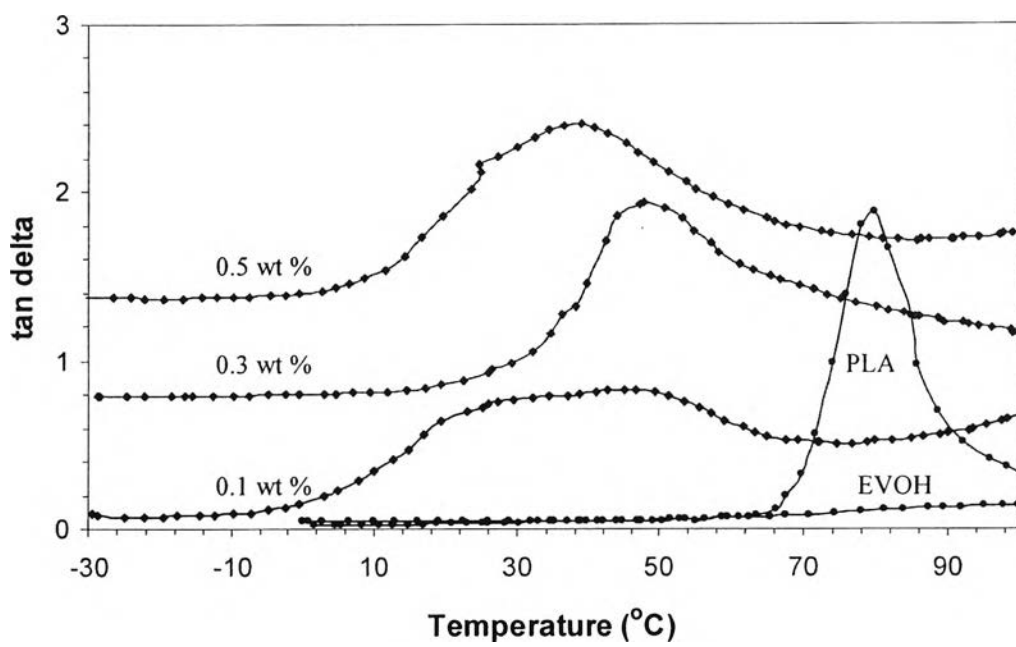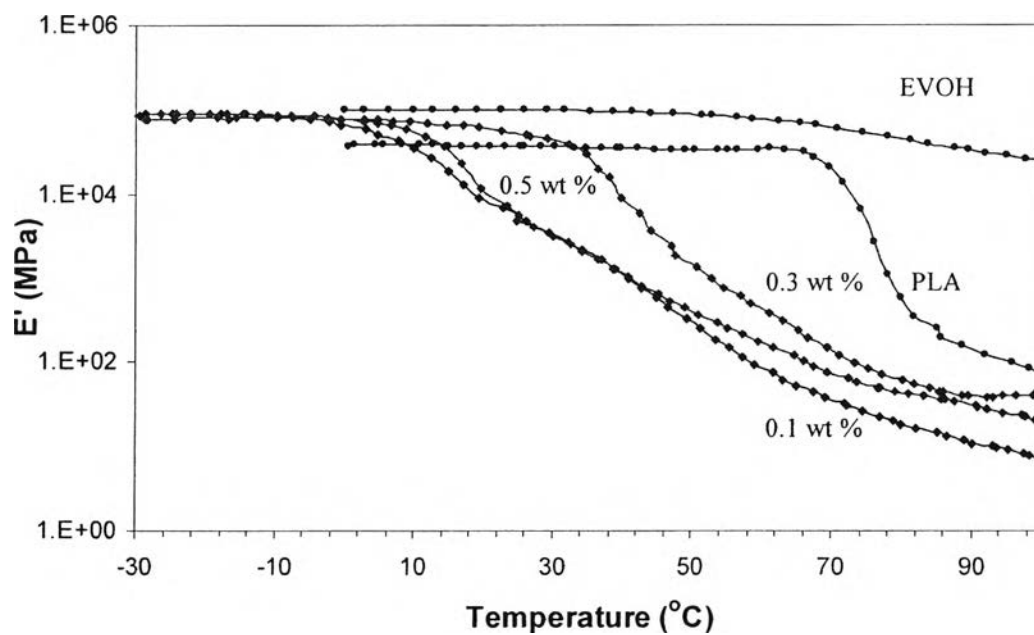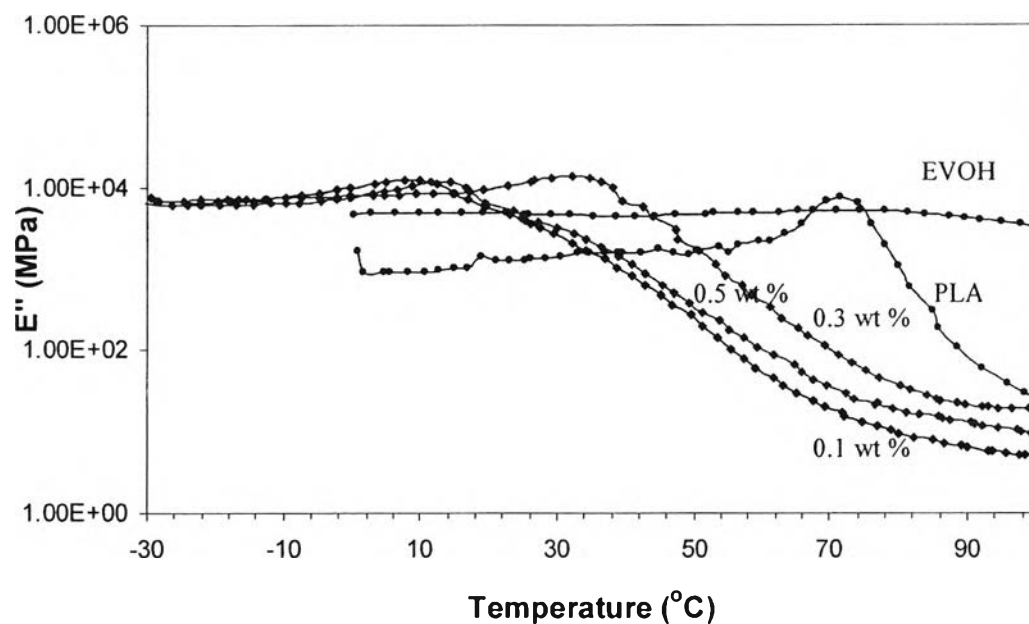
(a)



(b)

(c)

**Figure 4.24** DMA results of crude EVOH-g-PLA produced in reactive extrusion polymerization with 60/40 wt% LA/EVOH content, 0.1 wt% Sn(Oct)$_2$, and 5 wt% Zn/Ca stearate in dependence of screw speed (a) tan δ, (b) E', and (c) E'' as the function of temperature.

(a)



(b)

(c)

**Figure 4.25** DMA results of crude EVOH-g-PLA produced in reactive extrusion polymerization with 60/40 wt% LA/EVOH content, 5 wt% Zn/Ca stearate, and 30 rpm screw speed in dependence of catalyst content (a) tan δ, (b) E', and (c) E'' as the function of temperature.

### 4.4.8 Morphological characterization

Figures 4.26, 4.27, and 4.28 represent the scanning electron micrographs of the fractured surfaces of crude EVOH-g-PLA received in the catalytic extrusion. Figure 4.26 reveals the effect of LA/EVOH content on the morphology development, i.e. 50/50 and 60/40 wt% when homopolymer contents of PLA are minimized, show homogeneous surface, no pores, and some plastic yielding revealing good compatibility of the graft copolymer. However, tiny domains phase separation was seen in 50/50 wt% LA/EVOH graft copolymer. They are well distributed. 60/40 wt% LA/EVOH graft copolymer is well compatible so it is hardly seen the phase separation. 70/30 and 80/20 wt% LA/EVOH graft copolymers contains high amount of homopolymer of PLA and less amount of graft copolymer, so these samples have morphology look like blends of PLA and graft copolymer. Although their miscibility

is rather good due to one grass-transition temperature and phase separation with tiny domains, the adhesion between them is relatively poor as seen by poor distribution of the domains in 70/30 wt% LA/EVOH graft copolymer and domain splitting out and lefting holes in the 80/20 wt% LA/EVOH graft copolymer.
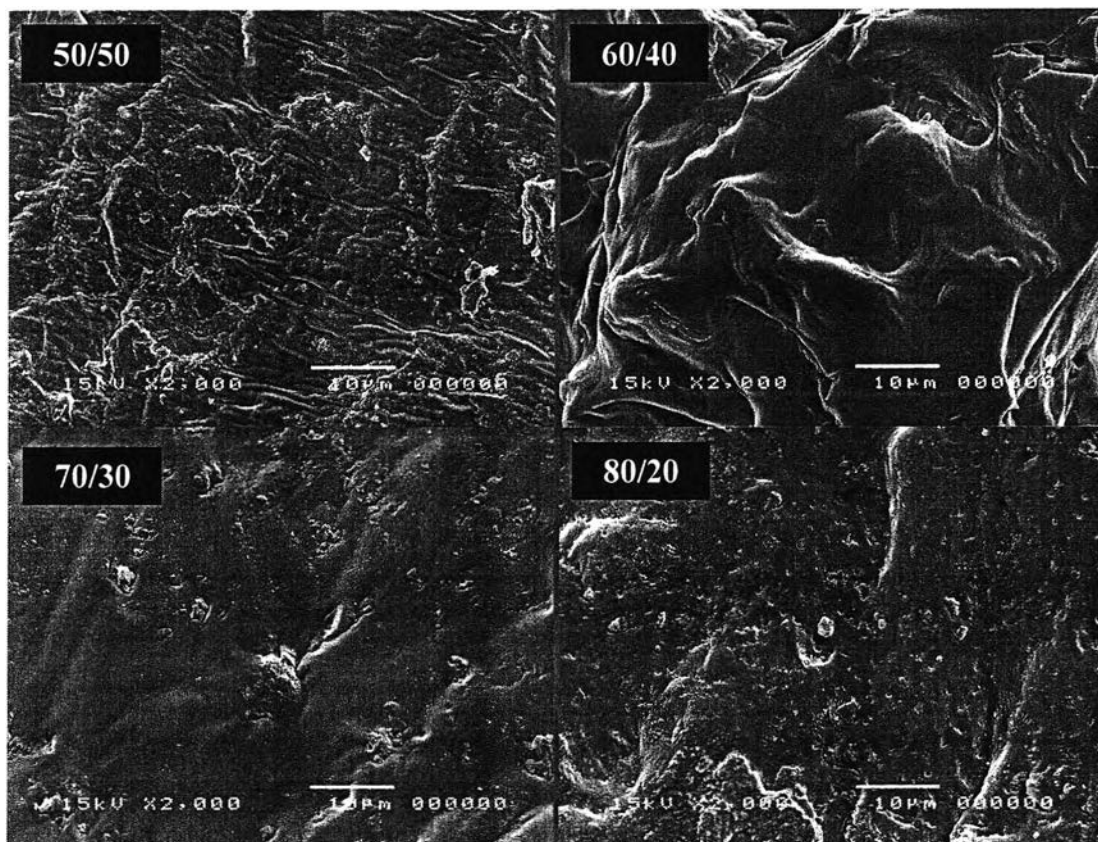


**Figure 4.26** SEM images of fractured surface of crude EVOH-g-PLA received in reactive extrusion polymerization at 40 rpm screw speed in dependence of LA/EVOH content.

For the most miscible copolymer 60/40 wt% LA/EVOH graft co-polymer, when the screw speed increases from 30 to 40 rpm the graft copolymer becomes homogeneous but for 50 and 60 rpm screw speed the mixing yields grain morphology that is brittle like structure due to less grafting content and more amount of homopolymer of PLA.
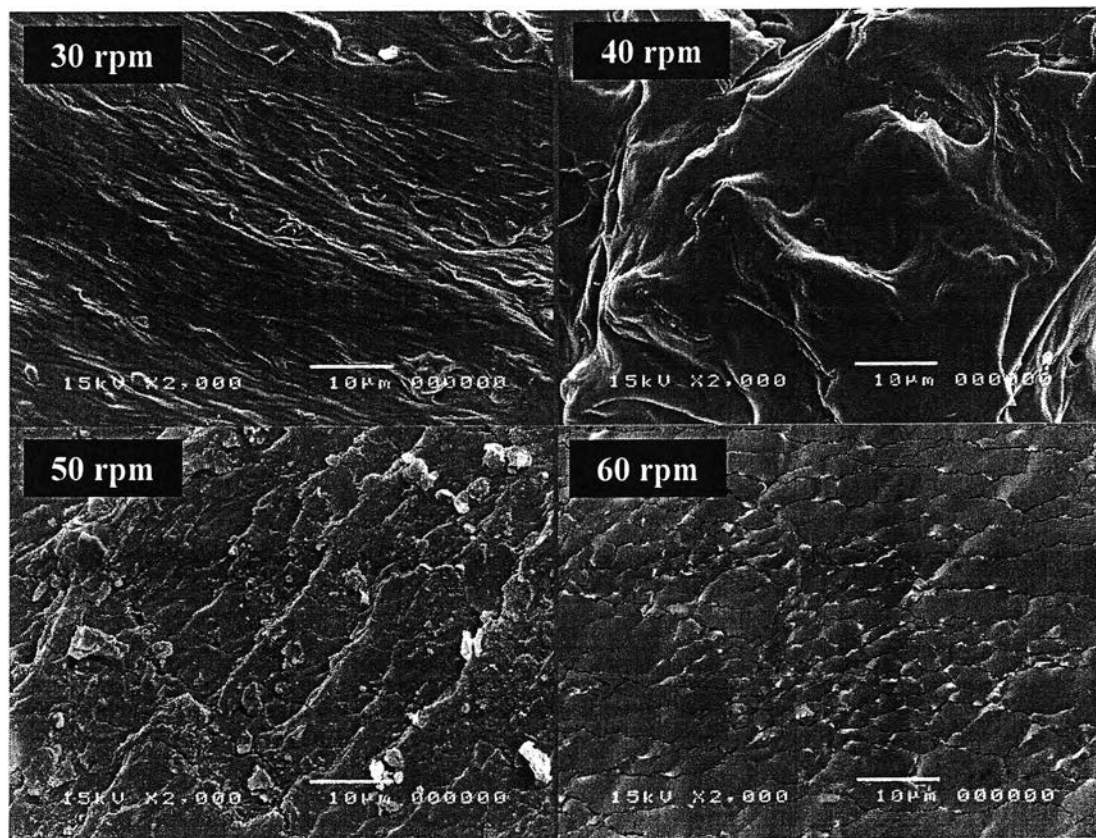
**Figure 4.27** SEM images of fractured surface of crude EVOH-g-PLA received in reactive extrusion polymerization with 60/40 wt% LA/EVOH content and 0.1 wt% catalyst content in dependence of screw speed.

Figure 4.28, the morphology of 0.1 wt% 60/40 wt% LA/EVOH graft copolymer produced at 30 rpm, when homopolymer of PLA is presented with significant amount of OH-grafting, shows more homogeneous and no phase separation. When catalyst content increases to 0.3 wt%, less homopolymer of PLA is formed but the OH-grafting degree is lower so the miscibility is poorer and the phase separation becomes obvious. At 0.5 wt% catalyst content, homopolymer of PLA is almost absence and grafting degree is high so no sign of holes but only phase separated with tiny domains.
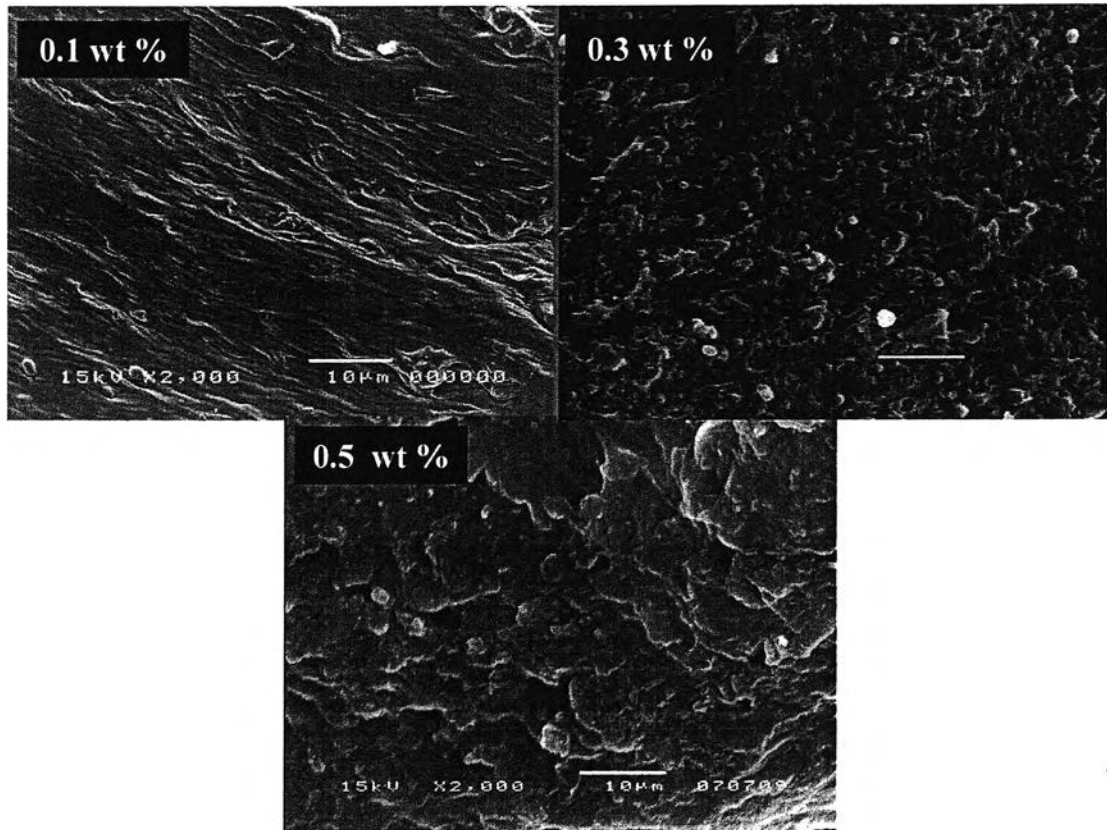
**Figure 4.28** SEM images of fractured surface of crude EVOH-g-PLA received in reactive extrusion polymerization with 60/40 LA/EVOH (wt%) at 30 rpm screw speed in dependence of catalyst content.

### 4.4.9 Mechanical behavior

Figure 4.29 reveals the different tensile behavior of crude graft copolymers compared to pure PLA and EVOH. The stress levels of pure PLA and EVOH were higher up to 40 MPa. In contrast to the graft copolymers, the elongation to break increased with the decrease in LA/EVOH content and screw speed and the increase in catalyst content. So, the PLA grafting-from EVOH shows decrease in stress and increase in the elongation to break.
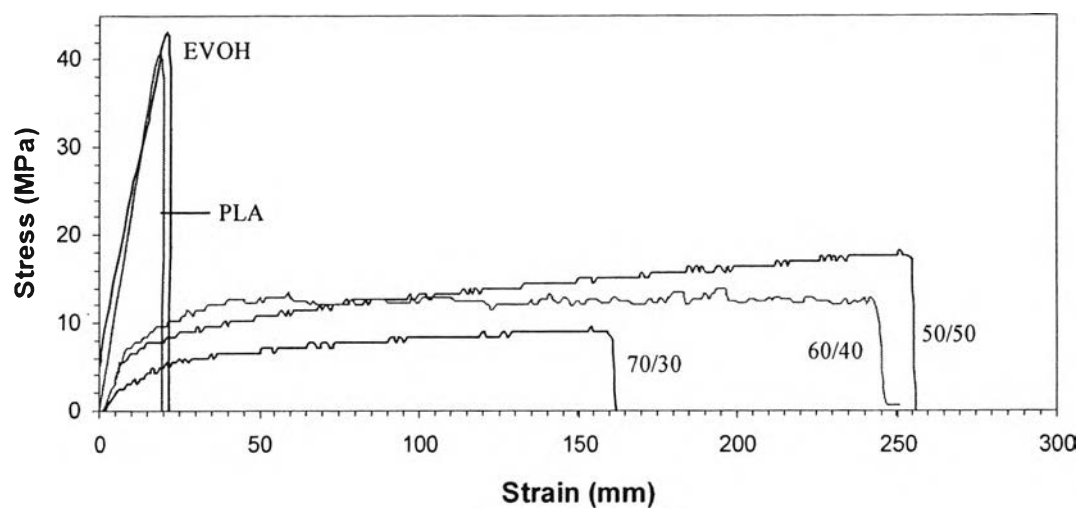
(a)
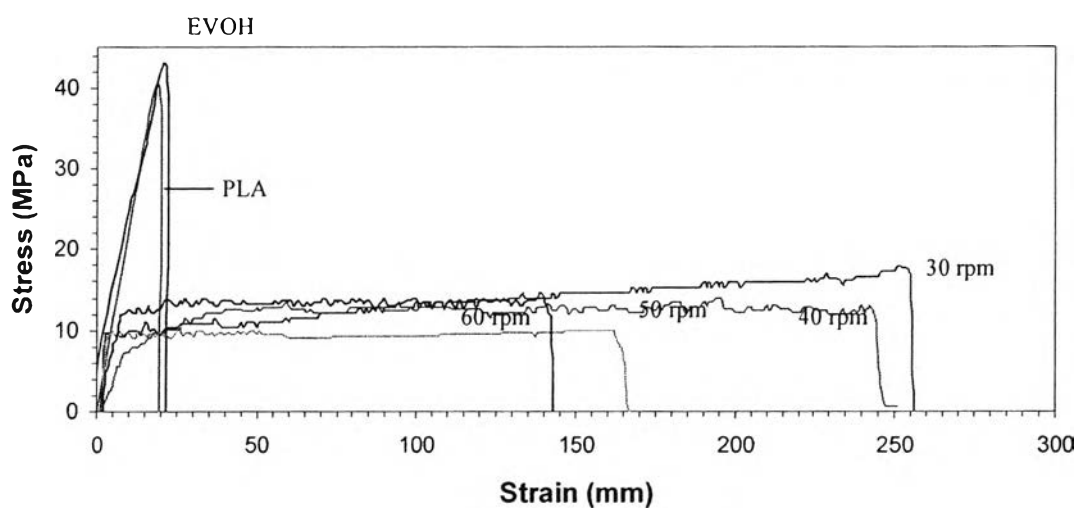


(b)
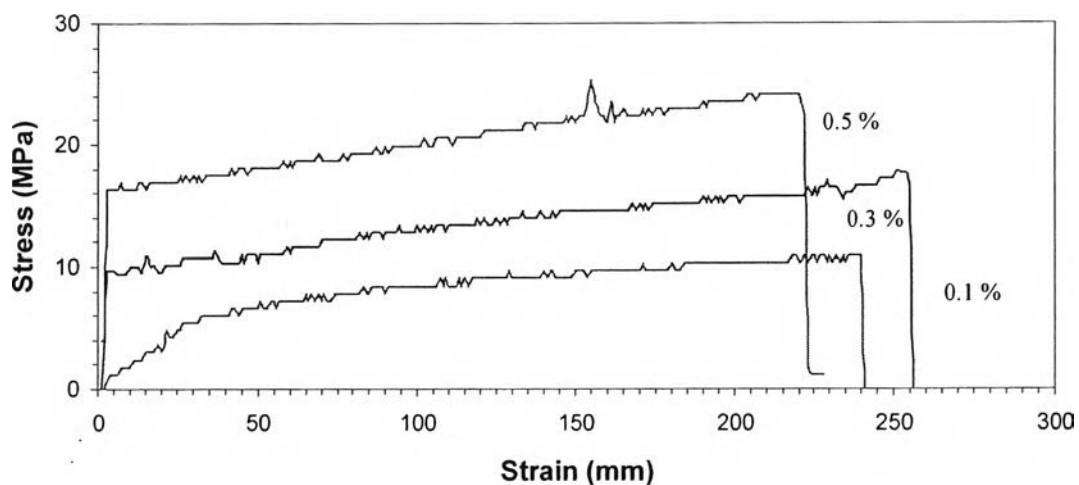
(c)

**Figure 4.29** Stress-strain curves of crude EVOH-g-PLA received in reactive extrusion polymerization in dependence of (a) LA/EVOH content, (b) screw speed, and (c) catalyst content.

**Table 4.7** Tensile strength of clude graft copolymers

| Samples | Tensile strength (MPa) | s.d. |
|---|---|---|
| **Commercial PLA** | 36.33 | 3.21 |
| **Commercial EVOH** | 40.00 | 2.83 |
| **LA/EVOH content (wt %)** | | |
| 50/50 | 17.75 | 1.06 |
| 60/40 | 11.50 | 0.71 |
| 70/30 | 9.00 | 1.41 |
| **Screw Speed (rpm)** | | |
| 30 | 15.00 | 1.41 |
| 40 | 11.50 | 0.71 |

| | | |
|---|---|---|
| 50 | 8.45 | 0.78 |
| 60 | 8.80 | 0.28 |
| Catalyst Content (wt %) | | |
| 0.1 | 15.00 | 1.41 |
| 0.3 | 17.00 | 1.41 |
| 0.5 | 21.50 | 0.71 |

**Table 4.8** Elongation at break of clude graft copolymers

| Samples | Elongation at break (%) | s.d. |
|---|---|---|
| Commercial PLA | 18.12 | 0.05 |
| Commercial EVOH | 18.64 | 1.93 |
| LA/EVOH content (wt %) | | |
| 50/50 | 230.87 | 2.64 |
| 60/40 | 228.69 | 8.43 |
| 70/30 | 150.08 | 3.32 |
| Screw Speed (rpm) | | |
| 30 | 238.87 | 8.68 |
| 40 | 228.69 | 8.43 |
| 50 | 149.46 | 2.06 |
| 60 | 132.63 | 1.65 |
| Catalyst Content (wt %) | | |
| 0.1 | 238.87 | 8.68 |
| 0.3 | 226.37 | 11.58 |
| 0.5 | 209.22 | 6.60 |

**Table 4.9** Young's modulus of clude graft copolymers

| Samples | Young's modulus (MPa) | s.d. |
|---|---|---|
| **Commercial PLA** | 194.55 | 22.05 |
| **Commercial EVOH** | 216.11 | 8.64 |
| **LA/EVOH content (wt %)** | | |
| 50/50 | 110.10 | 1.43 |
| 60/40 | 101.53 | 2.00 |
| 70/30 | 43.22 | 1.73 |
| **Screw Speed (rpm)** | | |
| 30 | 175.93 | 13.10 |
| 40 | 101.53 | 1.65 |
| 50 | 171.61 | 3.26 |
| 60 | 147.26 | 2.67 |
| **Catalyst Content (wt %)** | | |
| 0.1 | 175.93 | 13.10 |
| 0.3 | 439.06 | 7.62 |
| 0.5 | 495.57 | 72.45 |

Mechanical properties were determined by means of tensile testing. In this work, mechanical properties of crude EVOH-g-PLA obtained from the catalytic extrusion polymerization were compared with pure PLA and EVOH, especially tensile strength, elongation at break and Young's modulus. The analysis of the trends on mechanical properties gives information about the effect of LA/EVOH content, the screw speed, and the catalyst content. Figure 4.30 shows the tensile strength of the crude EVOH-g-PLA specimens in comparison with pure PLA and EVOH specimen. It was clearly seen that the tensile strength of all specimens received in the catalytic extrusion was smaller than that of pure PLA and EVOH. When the LA/EVOH content increased from 50/50 to 70/30 wt% and the reaction was carried out at the same screw speed (40 rpm), the tensile strength decreased due to the reduction of the mo-

lecular weight and poorer domain distribution. By varying the screw speeds from 30 to 60 rpm, the tensile strength decreased due to poorer domain distribution as well. The reason related to the residence time in the twin screw extruder. This resulted in the reduction of both grafting degree and molecular weight. Tensile strength significantly increased with catalyst content due to the increase in the molecular weight and high grafting content.
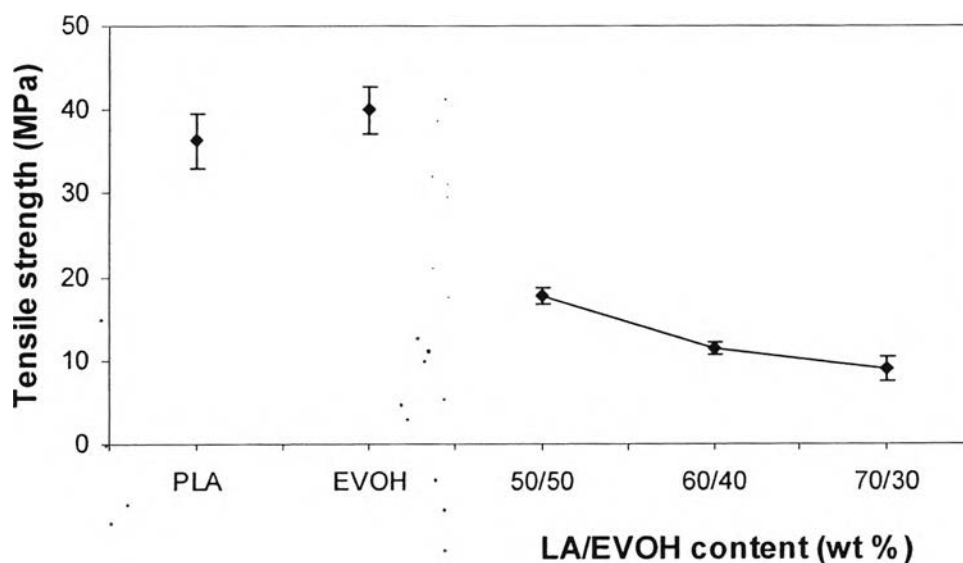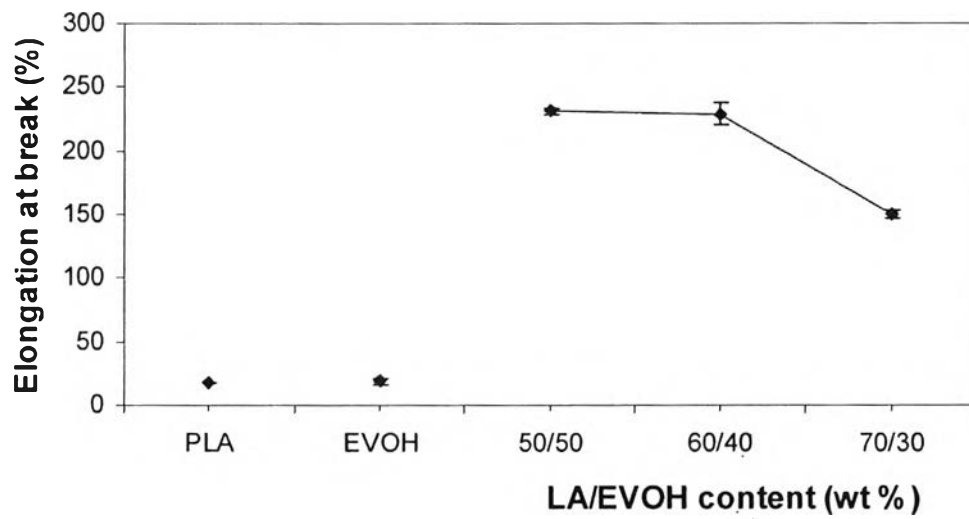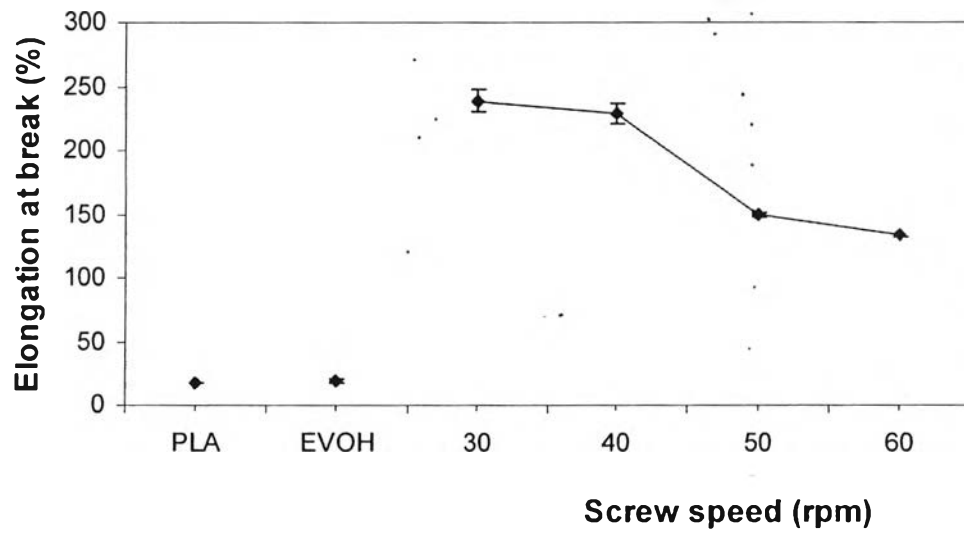


(a)
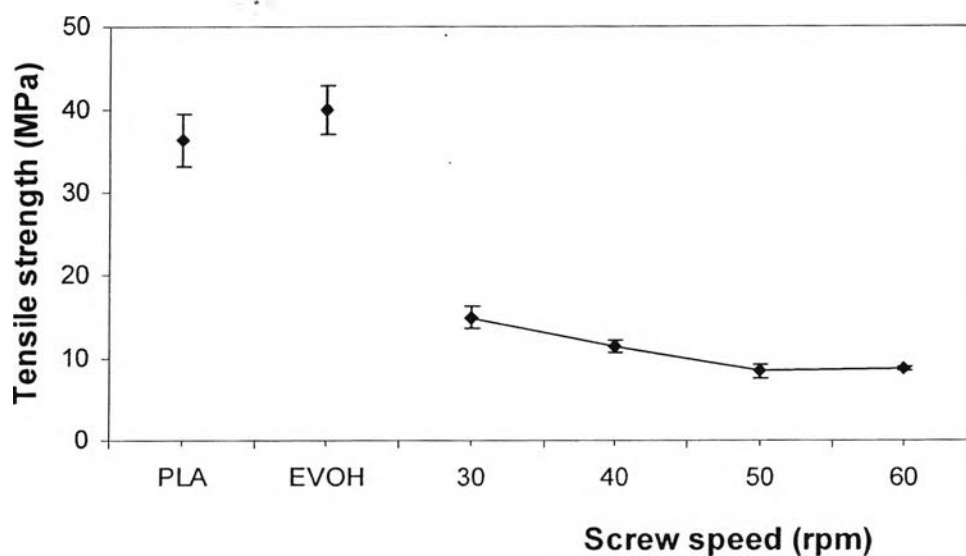


(b)
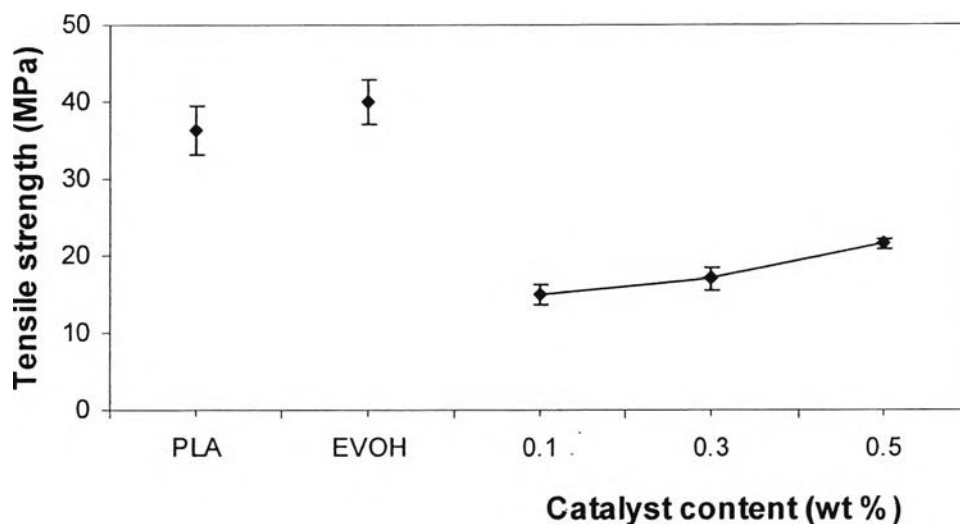
(c)

**Figure 4.30** Tensile strength of EVOH-g-PLA received in reactive extrusion po-
lymerization in dependence of (a) screw speed, (b) LA/EVOH content (wt%), and (c)
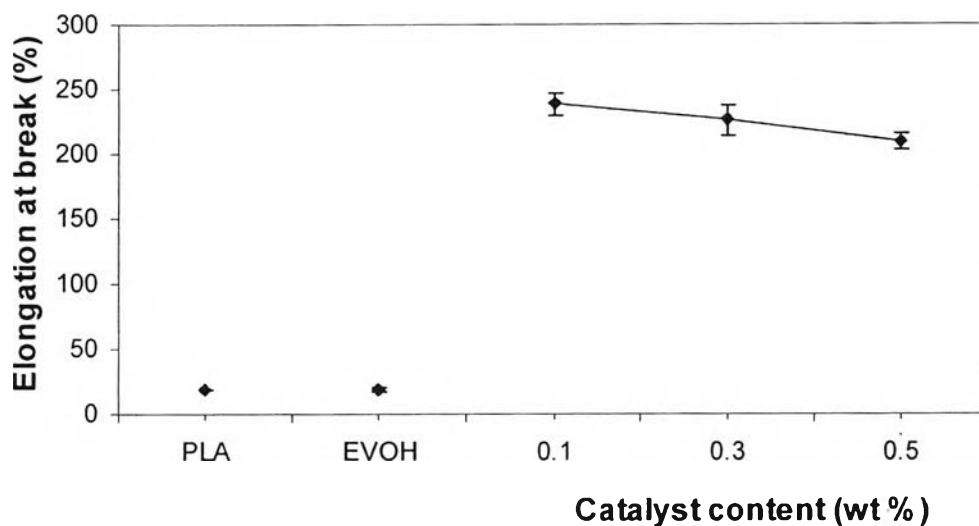catalyst content (wt%).

Elongation at break is shown in Figure 4.31. All of the crude EVOH-
g-PLA from the catalytic extrusion gave higher elongation at break compared to pure
PLA and EVOH. This could be suggested that the grafting of PLA from flexible
EVOH backbone improve the softness of PLA, so the brittle problem of PLA was
solved. When increasing the LA/EVOH contents from 50/50 to 70/30 wt%, there
was the decrease in the elongation at break as the function of LA/EVOH content.
The suggested reason was the same as the case of tensile strength. The specimens
obtained from different the screw speeds show the decrease in the elongation at
break decreased with increasing the screw speed. In the part of catalyst content varia-
tion, the elongation at break slightly decreased with increasing the catalyst content
from 0.1 to 0.5 wt%. Nevertheless, the difference in elongation at break of graft co-
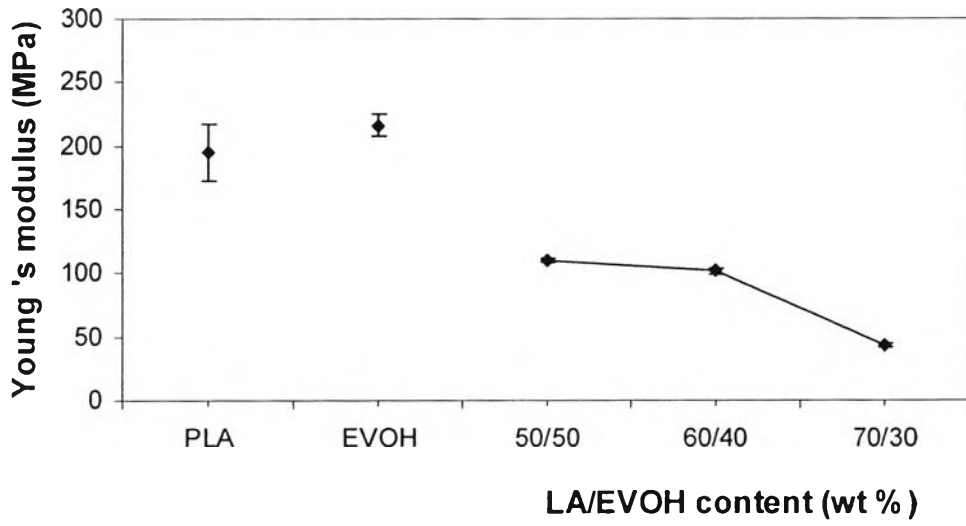polymers with various catalyst contents was very small.
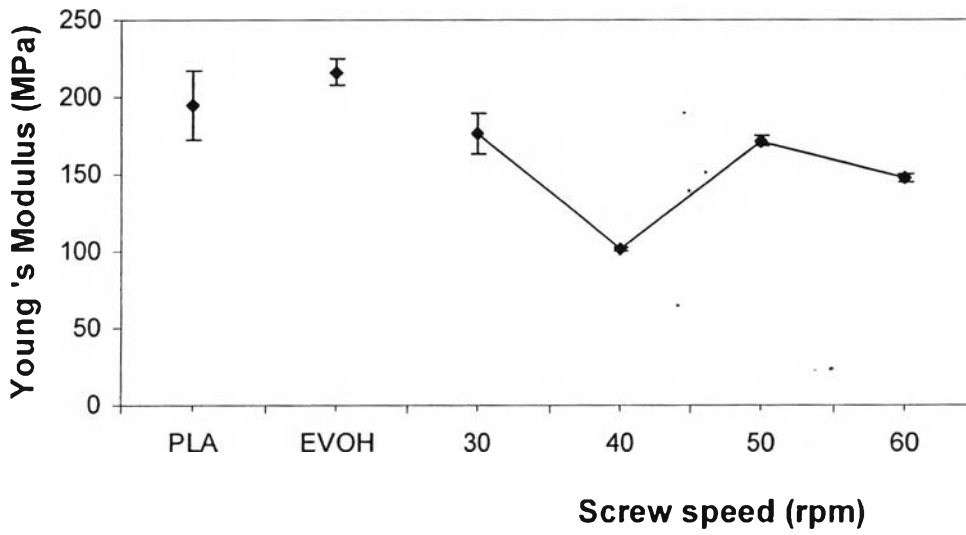
(a)



(b)

(c)

**Figure 4.31** Elongation at break of EVOH-g-PLA received in reactive extrusion po-lymerization in dependence of (a) screw speed, (b) LA/EVOH content (wt%), and (c) catalyst content (wt%).

Figure 4.32 shows the young's modulus of crude EVOH-g-PLA with various variables in comparison with pure PLA and EVOH. The graft copolymers gave the lower young's modulus than pure PLA and EVOH. This indicated that the grafting reduced the stiffness in comparison with pure PLA. The young's modulus of graft copolymers decreased when the LA/EVOH content was increased. In addition, it also decreased with increasing the screw speed. In the case of catalyst content variables, the young's modulus of graft copolymer changed linearly with the catalyst content. Particularly, graft copolymer with 0.5 wt% catalyst content showed very high young's modulus up to 500 MPa which was higher than that of pure PLA about two and half orders of magnitude.

(a)



(b)
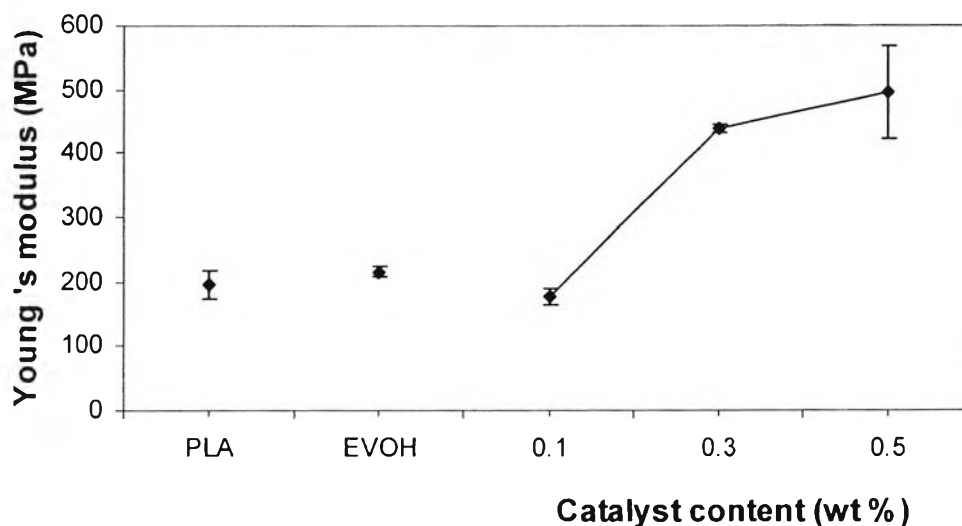
(c)

**Figure 4.32** Young 's modulus of EVOH-g-PLA received in reactive extrusion polymerization in dependence of (a) screw speed, (b) LA/EVOH content (wt%), and (c) catalyst content (wt%).

## 4.5 CONCLUSION

The brittleness of PLA was the starting point to use the catalytic extrusion for generating ring-opening polymerization of lactide and grafting from EVOH backbone in only single step. It was possible to synthesize PLA by grafting from method on EVOH via catalytic extrusion with stannous octoate as a catalyst which could be confirmed by the spectra of FTIR and NMR. The LA/EVOH content, extruder screw speed, and catalyst content are the important parameters which affected to the yield of graft copolymer, degree of grafting, molecular weight, and molecular weight distribution. The optimized LA/EVOH content, screw speed, and catalyst content were 60/40 wt%, 40 rpm, and 0.1wt%, respectively which based on the degree of grafting, monomer conversion, and their mechanical properties.

The glass-transition temperature of graft copolymers was lower in comparison with pure PLA and EVOH which both DSC and DMA gave the results in the same trend. From DSC curves and XRD patterns, all graft copolymers showed no crystal structure. It meant that high efficiency of grafting obstructed the crystalliza-

tion. In addition, from DMA results, $T_g$ of the graft copolymers was lower than that of pure PLA and EVOH. This decreased the rigidity and improved the processibility of PLA.

The grafting of PLA on EVOH backbone is to improve the elongation at break. The tradeoff includes reduced tensile strength. The mechanical properties related to the molecular weight of the graft copolymers. The graft copolymers which gave higher molecular weight showed better mechanical properties. The processibility was improved compared to that of pure PLA due to the high MWD.

## 4.6 ACKNOWLEDGEMENTS

## 4.7    REFERENCES

[1]    Jacobsen, S., Fritz, H.G., Degee, Ph., Dubois, Ph., and Jerome, R.  (2000). Polymer, 41, 3395-3403.

[2]    Yu, L., Dean, K., and Li, L. (2006). Progress in Polymer Science, 31, 576-602.

[3]    Luckachan, G. E., and Pillai, C.K.S. (2006). Carbohydrate Polymers, 64, 254-266.

[4]    Jacobsen, S., Fritz, H.G., Degee, Ph., Dubois, Ph., and Jerome, R.  (2000). Industrial Crops and Products, 11, 265-275.

[5]    Ana, M., Marcia, G., and Bluma, G.  (1997). Polymer Degradation and Stability, 58, 181-185.

[6]    Li, H., Jamshidi, and Huneault, M. A.  (2007).  Polymer, 48, 6855-6866.

[7]    Huang, M.H., Li, S., Vert, M.  (2004). Polymer, 45, 8675-8681.

[8]    Raquez, J.M., Degee, Ph., Nabar, Y., Narayan, R., and Dubois, Ph.  (2006). Comptes Rendus Chimie, 9, 1370-1379.

[9]    Huneault, M. A, and Li, H.  (2007).  Polymer, 48, 270-280.

[10] Jin, H.J., Chin, I.J., Kim, M.N., Kim, S.H., and Yoon, J.S. (2000). European Polymer Journal, 36, 165-169.

[11] Shi, D., Yang, J., Yao, Z., Wang, Y., Huang, H., Jing, W., Yin, J., and Costa, G. (2001). Polymer, 42, 5549-5557.

[12] Rosales, C., Marquez, L., Perera, R., and Rojas, H. (2003). European Polymer Journal, 39, 1899-1915.

[13] Zhu, L., Tang, G., Shi, Q., Cai, C., and Yin, J. (2006). Reactive & Functional Polymers, 66, 984-992.

[14] Eguiburu, J.L., Fernandez-Berridi, M.J., and Roman, J.S. (1996). Polymer, 37(16), 3615-3622.

[15] Vergnes, B. and Berzin, F. (2006). Comptes Rendus Chimie, 9, 1409-1418.

[16] Gopakumar, T.G., Ponrathnam, S., Lele, A., Rajan, C.R., and Fradet, A. (1999). Polymer, 40, 357-364.

[17] Ryner, M., Stridsberg, K., albertsson, A.C., Schenck, H., and Svensson, M. (2001). Macromolecule, 34, 3877-3881.

[18] Piao, L., deng, M., Chen, X., Jiang, L., and Jing, X. (2003). Polymer, 44, 2331-2336.

[19] Kelar, K. and Jurkowski, B. (2000). Polymer, 41, 1055-1062.

[20] Cartier, H. and Hu, G.H. (2001). Polymer, 42, 8807-8816.

[21] Moad, G. (1999). Progress in Polymer Science, 24, 81-142.

[22] Sutanto, P., Picchioni, F., Janssen, L.P.B.M. (2006). Chemical Engineering Science, 61, 7077-7086

[23] Odian, G. (2004). Principles of Polymerization. New Jersey: John Wiley & Sons.

[24] Schmack, G., Jehnichen, D., Vogel, R., Tandler, B., Beyreuther, R., Jacobsen, S., and Fritz, H.G. (2001). Journal of Biotechnology, 86, 151-160.

[25] Hyon, S.H., Jamshidi, K., and Ikada, Y. (1997). Biomaterials, 18, 1503-1508.

[26] Janata, M., Masar, B., Toman, L., Vlcek, P., Latalova, P., Brus, J., and Holler, P. (2003). Reactive & Functional Polymers, 57, 137-146.

[27] Lee, C. M., Kim, E. S., and Yoon, J. S. (2005). Published online in Wiley InterScience.

[28] Ren, Z., Dong, L., and Yang, Y. (2005). Published online in Wiley Inter-Science.